



**Andreia Filipa dos Santos Gomes**

Degree in Biochemistry

**Proteomic analysis of a  
neurodegeneration cell model, treated  
with plant extracts with potential  
neuroprotective activity**

Dissertation to obtain a Master Degree in Biotechnology

Supervisor: Cláudia Santos, Ph.D, IBET/ITQB-UNL

Co-Supervisor: Marta Alves, Ph.D, ITQB-UNL

Jury:

President: Professor Rui Oliveira, Ph.D.

Examiner: Gabriela Almeida, Ph.D.

Supervisor: Cláudia Santos, Ph.D.



FACULDADE DE  
CIÊNCIAS E TECNOLOGIA  
UNIVERSIDADE NOVA DE LISBOA

**September 2012**



**Andreia Filipa dos Santos Gomes**

Degree in Biochemistry

**Proteomic analysis of a neurodegeneration cell model,  
treated with plant extracts with potential  
neuroprotective activity**

Dissertation to obtain a Master Degree in Biotechnology

Supervisor: Cláudia Santos, Ph.D, IBET/ITQB-UNL  
Co-Supervisor: Marta Alves, Ph.D, ITQB-UNL

Jury:

President: Professor Rui Oliveira, Ph.D.

Examiner: Gabriela Almeida, Ph.D.

Supervisor: Cláudia Santos, Ph.D.



September 2012



Proteomic analysis of a neurodegeneration cell model, treated with plant extracts with potential neuroprotective activity

Copyright Andreia Gomes, FCT/UNL, UNL

A Faculdade de Ciências e Tecnologia e a Universidade Nova de Lisboa têm o direito, perpétuo e sem limites geográficos, de arquivar e publicar esta dissertação através de exemplares impressos reproduzidos em papel ou de forma digital, ou por qualquer outro meio conhecido ou que venha a ser inventado, e de a divulgar através de repositórios científicos e de admitir a sua cópia e distribuição com objetivos educacionais ou de investigação, não comerciais, desde que seja dado crédito ao autor e editor.

The Faculty of Science and Technology and the New University of Lisbon have the perpetual right, and without geographical limits, to archive and publish this dissertation through press copies in paper or digital form, or by other known form or any other that will be invented, and to divulgate it through scientific repositories and to admit its copy and distribution with educational or research objectives, non-commercial, as long as it is given credit to the author.



## Acknowledgments

All words will be few to express my gratitude to all who helped me in this stage of my life.

In special, I would like to thank to Cláudia Nunes dos Santos, PhD, and Marta Alves, PhD, my supervisors, for all the support, guidance and accuracy through this year. All this work would not have been possible without your help. You made me a better researcher and I'm so grateful for that.

To Professor Ricardo Boavida Ferreira, my sincere gratitude for having received me in the Disease and Stress Biology lab.

I would also like to express my gratitude to all the Disease and Stress Biology lab team, for the support and cooperation gave during this year, in particular to Inês Figueira and Lucélila Tavares. Thanks for all the laughs we took together. It was a pleasure working with you.

I cannot forget my family, especially my mother, father, César and Adriano for all the trust and for always believing in me. All I am I owe it to you. To all, thank you.

*“Failure teaches us that life is but a draft,  
an endless rehearsal of a show that will never play.”*

Le Fabuleux destin d'Amélie Poulain





## Abstract

Nowadays, a significant increase in chronic diseases is observed. Epidemiological studies showed a consistent relationship between the consumption of fruits and vegetables and a reduced risk of certain chronic diseases, namely neurodegenerative disorders. One factor common to these diseases is oxidative stress, which is highly related with proteins, lipids, carbohydrates and nucleic acids damage, leading to cellular dysfunction.

Polyphenols, highly abundant in berries and associated products, were described as having antioxidant properties, with beneficial effect in these pathologies.

The aims of this study were to evaluate by proteomic analyses the effect of oxidative insult in a neuroblastoma cell line (SK-N-MC) and understand the mechanisms involved in the neuroprotective effects of digested extracts from commercial and wild blackberry (*R. vagabundus* Samp.).

The analysis of the total proteome by two-dimensional electrophoresis revealed that oxidative stress in SK-N-MC cells resulted in altered expression of 12 protein spots from a total of 318.

Regarding some redox proteomics alterations, particularly proteins carbonylation and glutathionylation, protein carbonyl alterations during stress suggest that cells produce an early and late response; on the other hand, no glutathionylated polypeptides were detected.

Relatively to the incubation of SK-N-MC cells with digested berry extracts, commercial blackberry promotes more changes in protein pattern of these cells than *R. vagabundus*. From 9 statistically different protein spots of cells incubated with commercial blackberry, only  $\beta$ -tubulin and GRP 78 were until now identified by mass spectrometry.

Further studies involving the selection of sub proteomes will be necessary to have a better understanding of the mechanisms underlying the neuroprotective effects of berries.

**Keywords:** neurodegenerative diseases | polyphenols | digested berry extracts | cytoprotective effect | proteomics.



## Resumo

Nos dias de hoje assistimos a um aumento significativo das doenças crónicas. Estudos epidemiológicos mostraram uma relação consistente entre o consumo de frutas e vegetais e uma redução do risco de certas doenças crónicas, nomeadamente doenças neurodegenerativas. Um fator comum a estas doenças é o stresse oxidativo, que está relacionado com danos nas proteínas, lipídios, hidratos de carbono e ácidos nucleicos levando à disfunção celular.

Os polifenóis, muito abundantes em pequenos frutos e produtos associados, foram descritos como tendo propriedades antioxidantes com efeito benéfico nestas patologias.

Desta forma, este estudo teve como objetivos a avaliação do efeito do stresse oxidativo numa linha celular de neuroblastoma humano (SK-N-MC) e dos mecanismos envolvidos nos efeitos neuroprotetores de extratos digeridos de amoras comerciais e de uma variedade endémica (*R. vagabundus* Samp.) recorrendo à proteómica.

A análise do proteoma total por eletroforese bidimensional revelou que o stresse oxidativo imposto às células SK-N-MC promoveu a alteração de 12 *spots* proteicos num total de 318.

Em relação a algumas alterações redox nas células, particularmente carbonilação e glutationilação proteica, a resposta das proteínas carboniladas ao stresse ao longo do tempo sugerem que as células respondem de forma diferente no início e no final do período de stresse ao qual estão sujeitas. Por outro lado, não foram detetadas proteínas glutationiladas.

Relativamente à incubação das células SK-N-MC com extratos de amoras, a variedade comercial promove mais mudanças no padrão das proteínas do que a *R. vagabundus*. Dos 9 *spots* proteicos estatisticamente diferentes das células incubadas com amora comercial, apenas a  $\beta$ -tubulina e a GRP 78 foram identificados até agora através de espectrometria de massa.

Estudos adicionais envolvendo a seleção de subproteomas serão necessários para uma melhor compreensão dos mecanismos subjacentes aos efeitos neuroprotetores das amoras.

**Palavras-chave:** doenças neurodegenerativas | polifenóis | extratos digeridos de amoras | efeito citoprotetor | proteómica.



## General Index

<b>Acknowledgments</b> .....	vii
<b>Abstract</b> .....	ix
<b>Resumo</b> .....	xi
<b>General Index</b> .....	xiii
<b>Index of Figures</b> .....	xv
<b>Index of Tables</b> .....	xvii
<b>Abbreviations</b> .....	xix
<b>1. Objectives</b> .....	1
<b>2. Theoretical Fundamentals</b> .....	3
<b>2.1. Neurodegeneration</b> .....	3
2.1.1. Neurodegeneration and Oxidative Stress .....	3
2.1.2. Neurodegeneration and Berries .....	4
2.1.2.1. Bioavailability – <i>In vitro</i> Digestion .....	5
<b>2.2. Proteomics</b> .....	6
2.2.1. Total proteome analysis .....	6
2.2.2. Redox Proteomics .....	7
2.2.2.1. Protein carbonylation .....	8
2.2.2.2. Protein glutathionylation .....	9
<b>3. Material and Methods</b> .....	11
<b>3.1. Chemicals</b> .....	11
<b>3.2. Plant Material</b> .....	11
<b>3.4. <i>In vitro</i> digestion</b> .....	12
<b>3.5. Cell Culture</b> .....	12
<b>3.6. Time course profile of cells incubated with hydrogen peroxide</b> .....	12
<b>3.7. Incubation of cells with digested plant extracts</b> .....	13
<b>3.8. Protein Quantification</b> .....	13
<b>3.9. Electrophoresis</b> .....	13
3.9.1. 1D Electrophoresis .....	13
3.9.2. 2D Electrophoresis .....	14
3.9.3. Gel Staining .....	14
3.9.3.1. Coomassie Brilliant Blue .....	14
3.9.4. 2DE Gel analysis .....	15
<b>3.10. Mass spectrometry analysis</b> .....	15
<b>3.11. Western Blot</b> .....	16

3.11.1.	Electrotransfer of polypeptides .....	16
3.11.2.	Ponceau S Staining.....	16
3.11.3.	Immunodetection.....	17
3.12.	Measurement of glutathione released from glutathionylated proteins .....	17
3.13.	Statistical Analysis .....	18
<b>4.</b>	<b>Results and Discussion .....</b>	<b>21</b>
<b>4.1.</b>	<b>Evaluation of Oxidative Stress .....</b>	<b>21</b>
4.1.1.	Time course profile of protein extracts from SK-N-MC cells treated with hydrogen peroxide .....	21
4.1.2.	Protein Carbonyls .....	27
4.1.3.	Protein S-Glutathionylation.....	29
<b>4.2.</b>	<b>Protein pattern of SK-N-MC cell line treated with different digested berry extracts... ..</b>	<b>32</b>
<b>5.</b>	<b>Final considerations and future perspectives .....</b>	<b>41</b>
<b>6.</b>	<b>Bibliography .....</b>	<b>43</b>
<b>7.</b>	<b>Annexes .....</b>	<b>49</b>

## Index of Figures

<b>Fig. 2.1</b> - Representative scheme of the <i>in vitro</i> digestion model, adapted from Aura A. M. and McDougall G. J, <i>et al.</i> [28, 29].....	5
<b>Fig. 2.2</b> - Involvement of oxidative stress in the pathophysiology of cells, adapted from Radak, Z., <i>et al.</i> [48].....	8
<b>Fig. 4.1</b> - (A) Representative 2DE control gel of SK-N-MC cells (65 µg).The gel was CBB stained. Twelve spots were found to change quantitatively between the control and stress conditions evaluated (0-24 h), and numbered spots have been sent for protein identification by MS; (i) Zoom in of some protein spots of 2DE gel with high contrast; (B) Comparison of protein spots differentially expressed against control, white columns for upregulated proteins and gray column for downregulated protein spots. ....	22
<b>Fig. 4.2</b> - (A) Protein carbonyl profile of SK-N-MC cells submitted to oxidative injury (300 µM H <sub>2</sub> O <sub>2</sub> ) with different times of exposure (0-24 h), in comparison to control (CTRL), as well as oxidized BSA (Ox. BSA – positive control); (B) immunodetection of the loading control (β-actin). Protein carbonyl profile was obtained after sample derivatization using OxyBlot™ Protein Oxidation Detection kit (Interger) Western blot was exposed to chemiluminescence detection using FemtoMax Super Sensitive Chemiluminescent HRP Substrate – Rockland Inc. A representative image is shown.....	28
<b>Fig. 4.3</b> - Protein glutathionylation profile of SK-N-MC cells submitted to oxidative injury (300 µM H <sub>2</sub> O <sub>2</sub> ) with different times of exposure (0-24 h), in comparison to (A) control (CTRL), as well as (B) oxidized samples with 5 mM GSSG. Glutathionylated protein profile was obtained after incubation with mouse anti-GSH antibody (Virogen). Western blot was exposed to chemiluminescence detection using FemtoMax Super Sensitive Chemiluminescent HRP Substrate – Rockland Inc. A representative image is shown.....	30
<b>Fig. 4.4</b> - Representative 2DE control gel of SK-N-MC cells. The gel was CBB stained. One protein spot (white spot) from SK-N-MC cells incubated with <i>R. vagabundus</i> (RV) during 24 h and 9 protein spots (black spots) from SK-N-MC cells incubated with commercial blackberry (BB) during 24 h were statistically different from control. Numbered spots were sent for protein identification by MS. ....	33
<b>Fig. 4.5</b> - Time course profile for the expression of GRP 78 in SK-N-MC cells when incubated for different periods of time (0-24 h) with 300 µM H <sub>2</sub> O <sub>2</sub> . ....	39
<b>Fig. 4.6</b> - Scheme of the hypothetical effect of commercial blackberry (A) and <i>R.vagabundus</i> digested extracts (B) in caspases and GRP 78 expression in SK-N-MC cells. ....	40

**Fig. S1** - Thiols time course profile of stressed SK-N-MC cells: GSH. SK-N-MC cells were submitted to an oxidative stress (300 $\mu$ M H<sub>2</sub>O<sub>2</sub>) for different incubation periods (0-24 h) and protein cellular extracts were derivatized and quantified by HPLC with fluorescence detector. Glutathione-OPA adduct was monitored at excitation and emission wavelengths of 350 and 420 nm, respectively. Quantifications of GSH were normalized for total protein content. Represented values are the averages  $\pm$  S.D. of at least three independent determinations. Differences between treatments in relation to control are denoted as \* $p$ <0.05 \*\* $p$ <0.01. Data provided by a colleague from DSB Lab. .... 49

**Fig. S2** - (A) Caspase-3 and -7 activity from SK-N-MC cells when incubated with 0.5  $\mu$ g GAE mL<sup>-1</sup> of commercial blackberry (BB) or *R.vagabundus* (RV); Differences between treatments in relation to control (CTRL) are denoted as \* $p$ <0.05 \*\* $p$ <0.01 (B) Caspase-3 and -7 activity from SK-N-MC cells when pre-incubated with 0.5  $\mu$ g GAE mL<sup>-1</sup> of commercial blackberry (BB) or *R.vagabundus* (RV) and then submitted to oxidative stress (300  $\mu$ M H<sub>2</sub>O<sub>2</sub>); Differences between treatments in relation to oxidative stress (Stress) are denoted as \*\* $p$ <0.01. Data provided by a DSB Lab colleague. .... 49



## Index of Tables

<b>Table 3.1</b> - Antibodies and dilutions used in Western blot analyses. ....	17
<b>Table 4.1</b> - Time course profile for the expression of protein spots differentially expressed in SK-N-MC cells treated with 300 $\mu$ M H <sub>2</sub> O <sub>2</sub> and their characteristics (pI and MW (kDa)). Differences between treatments in relation to control are denoted as * $p$ <0.05 ** $p$ <0.01, *** $p$ <0.001.....	23
<b>Table 4.2</b> - HPLC chromatograms of GSH and GSSG for SK-N-MC cells incubated with H <sub>2</sub> O <sub>2</sub> (300 $\mu$ M) during 4 h and HPLC chromatograms for GSH released from glutathionylated proteins (PSSG) relatively to SK-N-MC control cells (0 h). Glutathione-OPA adduct was monitored at excitation and emission wavelengths of 350 and 420 nm, respectively.....	31
<b>Table 4.3</b> - Normalized volumes for protein spots in SK-N-MC cells treated with commercial blackberry (BB) and <i>R. vagabundus</i> (RV) differentially expressed from control (CTRL) and their characteristics (pI and MW (kDa)). Differences between treatments in relation to control are denoted as * $p$ <0.05 ** $p$ <0.01 *** $p$ <0.001. ....	34
<b>Table 4.4</b> - Protein identification by MS/MS and respectively gel images for control (CTRL) and commercial blackberry (BB). ....	38



## **Abbreviations**

**1DE** – One Dimensional Electrophoresis;

**2DE** – Two-dimensional electrophoresis;

**3-NT** - 3-Nitrotyrosine;

**AD** – Alzheimer’s Disease;

**ANOVA** – Analysis of Variance;

**BB** – digested extracts from commercial blackberry;

**BSA** – Bovine Serum Albumine;

**CBB** – Commassie Brilliant Blue;

**CDI** – Collision-Induced Dissociation;

**CHAPS** – 3[(3-Cholamidopropyl)dimethylammonio]-propanesulfonic acid;

**CNS** – Central Nervous System;

**CTRL** – Control;

**DNP** – 2,4-Dinitrophenylhydrazine;

**DNPH** – 2,4-Dinitrophenylhydrazine;

**DTT** – Dithiothreitol;

**EDTA** – Ethylenediamine Tetra-Acetic Acid;

**EMEM** – Eagle Minimum Essential Medium;

**FBS** – Fetal Bovine Serum;

**GAE** – Gallic Acid Equivalents;

**GI** – Gastro Intestinal;

**GSH** – Glutathione;

**GSSG** – Glutathione disulfide;

**HNE** - 4-hydroxy-2-*trans*-nonenal;

**HPLC** – High Performance Liquid Chromatography;

**HRP** – Horseradish Peroxidase;

**HSD** – Honest Significant Difference;

**IEF** – Isoelectric Focusing;

**IVD** – *In vitro* Digestion;

**MALDI** – Matrix-Assisted Laser Desorption/Ionization;

**MS** –Mass Spectrometry;

**MS/MS** – Mass Spectrometry/Mass Spectrometry;

**MTs** – Microtubules;

**MW** – Molecular Weight;  
**NEM** – *n*-Ethylmaleimide;  
**NOS** – Nitrosative Oxygen Species;  
**OPA** – Orthophthaldehyde;  
**ORAC** – Oxygen Radical Absorbance Capacity;  
**PBS** – Phosphate Buffer Saline;  
**PD** – Parkinson's disease;  
**pI** – Isoelectric Point;  
**PSH** – Protein Sulfidryl groups;  
**PSSG** – Protein *S*-glutathionylated;  
**PTM'S** – Pos-translational Modifications;  
**PVDF** – Polyvinylidene Fluoride  
**ROS** – Reactive Oxygen Species;  
**RV** – digested extracts from *Rubus vagabundus* Samp;  
**SAF** – Serum Available Fraction;  
**SDS-PAGE** – Sodium Dodecyl Sulphate-Polyacrylamide Gel Electrophoresis;  
**TOF/TOF** – Time-of-Flight;

## 1. Objectives

Neurodegenerative disorders are an increasing concern of the World's population. Understanding the mechanisms underlying the development of these disorders is a crucial step in the quest for alternative therapies or even in the prevention of these diseases.

Recently, berries upsurge as potential functional foods in the prevention of neurodegenerative diseases.

In order to have insights of the metabolic pathways involved in oxidative stress responses and neuroprotective effect of digested berry extracts (commercial blackberry and *R. vagabundus*) an *in vitro* cell model will be used to: i) study the alterations that occur in the total proteome, protein carbonylation and glutathionylation of a neurodegeneration cell model, which uses SK-N-MC cells submitted to oxidative injury; and ii) study the alterations that occur in the total proteome of the human neuroblastoma SK-N-MC cells incubated with digested berry extracts. A detailed analysis of the protein profiles obtained using appropriate software for image analyses should be performed to pinpoint the polypeptides that respond to the conditions imposed to the cells. The identification of those polypeptides will contribute to the overall understanding of our neurodegeneration cell model and neuroprotective effects that digested berry extracts exert in this model.



## 2. Theoretical Fundamentals

### 2.1. Neurodegeneration

Neurodegeneration may be a consequence of various forms of neural cell death, e.g. necrosis and apoptosis. These forms of cell death may result from a variety of cellular insults, including excitotoxicity and oxidative stress [1-3]. Commonly, neurodegeneration is defined by the progressive loss of specific neuronal cell populations and is associated with protein aggregates. Alzheimer's disease (AD) is the most common age-associated neurodegenerative disorder; is characterized by dementia, cognitive impairment and memory loss, which in the near future will affect around 22 million persons in the world [4-6]. AD is characterized by the accumulation of extracellular amyloid- $\beta$  deposited in senile plaques, and intracellular neurofibrillary tangles composed principally of abnormal and hyperphosphorylated tau protein [7].

The second most common neurodegenerative disorder affecting elderly people is Parkinson's disease (PD). The patients suffer from progressive loss of dopaminergic neurons in basal ganglia and the *substantia nigra*, which entails a substantial decrease of the neurotransmitter dopamine [8].

AD and PD are all major neurodegenerative disorders where oxidative stress is implicated. Many proteomic studies have provided confirmation of the oxidative damage of particular proteins in these diseases [3, 9].

#### 2.1.1. Neurodegeneration and Oxidative Stress

Oxidative stress can induce neuronal cell death in a variety of circumstances and is a condition in which the imbalance of reactive oxygen species (ROS) and reactive nitrosative species (NOS) production and the level of antioxidants are significantly disturbed resulting in damage to cells [3, 10]. Indeed, ROS/NOS are able to modulate the function of biomolecules causing protein, DNA, RNA oxidation, or lipid peroxidation contributing for the progression of neurodegeneration [10]. Compared to DNA and lipids, proteins are the most abundant cellular targets for oxidation [11]. Therefore, protein oxidation may disrupt cellular functions by altering protein expression, gene regulation, protein turnover and modulation of cell signaling, among others alterations. Typical oxidative modifications of brain proteins involve carbonyls, protein-bound 4-hydroxy-2-trans-nonenal (HNE) and 3-nitrotyrosine (3-NT), thiol groups oxidation and glutathionylation [8].

Central Nervous System (CNS) is said to be especially sensitive to oxidative stress because it presents high oxygen (O<sub>2</sub>) consumption leading to the production of free radicals; unexpectedly

it is relative deficient in the enzymes that metabolize a number of oxygen-based reactants to innocuous species, and highly enriched in polyunsaturated fatty acids which are readily oxidized by toxic oxygen derivatives [12, 13].

In our lab, Disease and Stress Biology (DSB) Lab, SK-N-MC cell line is used as a human neuronal cell model. It is a clonal neuroblastoma cell line composed of small fibroblast-like cells which contain a reduced cytoplasm. This is a continuous cell line, obtained from human metastatic neuroblastoma tissue [14]. Cellular models may have some limitations but they are a very helpful way to try to reproduce and manipulate molecular mechanisms that can be extrapolated for whole organisms, offering a faster approach to get solid results and providing valuable biochemical information.

To create a neurodegeneration cell model, cultured SK-N-MC are exposed to relatively low concentration of hydrogen peroxide ( $H_2O_2$ ) that induces changes in cell metabolism leading to some neuronal cell death, mimicking what may occur during neurodegeneration [15].

#### 2.1.2. Neurodegeneration and Berries

Berries are rich sources of a wide variety of antioxidant phenolics such phenolic acids, flavonoids, stilbenes and tannins, which are associated with many biologically significant mechanism of action, like scavenging and detoxification of ROS [16].

The importance of the diet in relation to human health has increased the interest of consumers about rich diets, which include fruits and vegetables [16].

Epidemiological studies have shown a consistent relationship between the consumption of fruits and vegetables and a reduced risk of certain chronic diseases such as neurodegenerative disorders. In particular, berries and associated products have an increasing focus of attention, not only because of its high nutritional value and beneficial effects to human health, but also because they are crops with agro-economic importance [17-19].

Some *in vitro* studies demonstrate a potent antioxidant, antiproliferative and anti-inflammatory activities of blackberry; moreover studies with rodents have revealed an attenuation of brain aging when these fruits are ingested [20-22].

Recent studies revealed that endemic blackberry species of the Northeast of Portugal, as for instance *Rubus brigantinus* and *Rubus vagabundos* Samp., are promising sources of polyphenols that are able to protect neuronal cells from oxidative injury, one of the most important characteristics in neurodegeneration [23]. However, for the understanding of the mechanisms underlying these beneficial effects, it is necessary to have in consideration the bioavailability of these berry polyphenols in the human body [24-26].



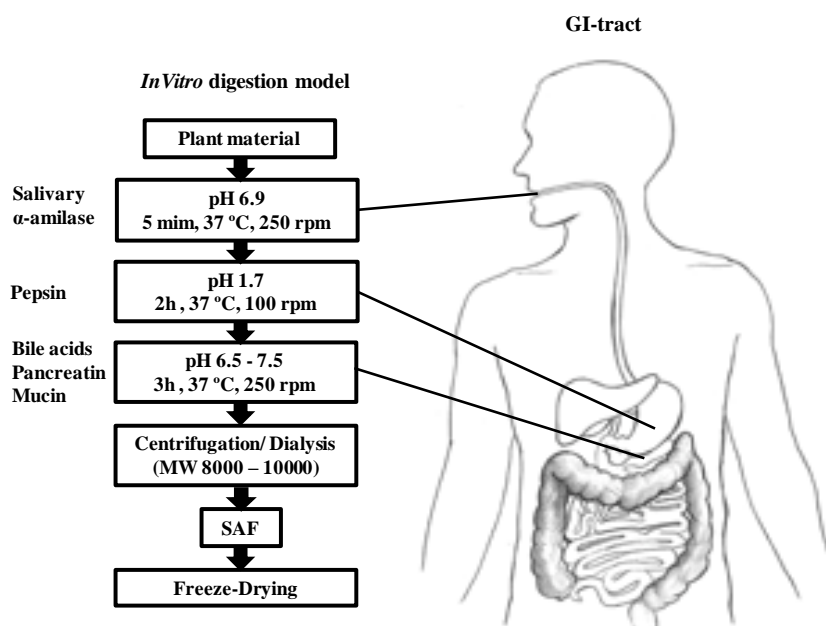
#### 2.1.2.1. Bioavailability – *In vitro* Digestion

The health effects of phenolic compounds are largely dependent upon their bioavailability. The commonly accepted definition of bioavailability is the proportion of the polyphenols that is digested, absorbed and metabolised. Consequently, it is not only important to know how much of a polyphenol is present in a food or dietary supplement, but even more important to know how much of that is bioavailable, *i.e.* the quantity of polyphenols that reach the target tissue [27].

Various studies established that the chemical structure of phenolics reaching the peripheral circulation and tissues differ from those present in foods, due to the biotransformation in the gastrointestinal tract (GI) [24]. Since the GI-tract is a barrier of access of phytochemicals to other organs, the use of an *in vitro* digestion procedure provides a simple and rapid method to assess the potential stability of phytochemicals from fruits [28].

In order to understand the mechanisms underlying the neuroprotection of digested berry polyphenols, we used a *in vitro* digestion model (IVD) that simulates the physicochemical and biochemical changes that occur in the GI-tract (Fig. 2.1) [28].

Serum available fractions (SAF) from commercial blackberry (BB) and *R. vagabundus* Samp. (RV) obtained by IVD were used in the neurodegeneration cell model to evaluate the mechanisms involved in the neuroprotective effects of these two species by using proteomic analyses.



**Fig. 2. 1** - Representative scheme of the *in vitro* digestion model, adapted from Aura A. M. and McDougall G. J, *et al.* [28, 29]

## 2.2. Proteomics

The knowledge gathered so far indicate that proteins are involved in almost all biological activities meaning that the study of the proteome of a cell or organism can contribute to the understanding of biological systems [30, 31]. As in the case of the understanding of disorders in the nervous system, where proteomic approaches are being successively used.

The comparative analysis of cerebral disorders such AD and PD is one of many examples where proteomics plays an important role [8].

Several technologies can be used in proteomic research being the gel-based applications (one and two-dimensional polyacrylamide gel electrophoresis (1DE or 2DE)) one of the most commonly used approaches [32-35]. However, for the characterization of a complex proteome a combination of different proteomic approaches can be used [31].

Nevertheless, proteomic research is still dealing with some difficulties due the origin and complexity of the protein extract, physical and chemical properties of certain proteins and instrumental limitations. Therefore, proteomics is an ongoing and developing field with the existing technologies being still further improved [36].

### 2.2.1. Total proteome analysis

An ideal separation method would be able to resolve, in a single map, all of the proteins expressed by a single cell. Current technologies, however, have not achieved this resolution yet, and nowadays the only available technique that provides a global profile of a cell proteome is high resolution two-dimensional electrophoresis (2DE) [37]. This technique was developed during the 1970s, and is the first approach and probably still the most frequently used technique to separate complex protein mixtures prior to downstream protein characterization by mass spectrometry (MS) [4, 31, 36, 38, 39]. The 2DE is based on two important physicochemical properties of the polypeptides: isoelectric point (pI), the specific pH at which the net charge of the protein is zero, and molecular weight (MW) [4].

Protein spots on 2DE gels can be visualized by a variety of protein staining techniques, each with specific technical aspects, sensitivity, linear range for quantification, reproducibility and compatibility with mass spectrometry [36] .

After 2DE gel image acquisition analysis by specialized software is performed. These software's are used for spot detection, spot matching, and comparison of spot intensities among several gels [36]. Then the protein spots of interest can be identified by MS. This technique represents one of the most important tools in proteomics, because presents a short time analysis, high sensitivity, feasibility and automation.

### 2.2.2. Redox Proteomics

Redox proteomics approaches aims to identify oxidatively modified proteins such as protein carbonyls, 3-NT-, and HNE-modified proteins in various biological samples in redox signaling scenarios and oxidative stress [40-43].

Oxidatively modified proteins can have repercussions at both physiological and pathological levels [43-45]. One consequence of protein oxidation can be conformational changes, thereby leading to exposure of the hydrophobic amino acids residues to an aqueous environment, promoting protein aggregation and accumulation of the oxidized proteins as cytoplasmatic inclusions. Another consequence can be the loss of tertiary structure of a protein consequently affecting its function [8, 42].

Some amino acids like lysine, arginine, proline and threonine side-chains can be oxidatively converted to reactive aldehyde or ketone groups causing inactivation, cross-linking or breakdown of proteins. Also sulphur-containing residues, cysteine and methionine, are especially susceptible to oxidation, and cysteines can be also oxidized forming disulfides in proteins or as mixed disulfides with cysteine or GSH (Fig. 2.2) [46, 47].

In redox proteomics approaches the same principles for separation and identification of proteins are employed, however a 2DE Western Blot is used in complement to immunochemically detect oxidatively modified proteins [40, 41].

Redox proteomics methods for the detection of protein carbonylation and glutathionylation allowed the identification of various oxidatively modified brain proteins in a variety of neurodegenerative disorders or associated models, providing new insights to the mechanisms of these diseases, namely identification of associated markers. The identification of oxidatively modified proteins, especially in neurodegenerative diseases is the ongoing pursuit of redox proteomics [40].



#### 2.2.2.2. Protein glutathionylation

The thiol redox state can also be used to reflect the oxidant conditions in a biological system. Thiols have numerous functions, including a central role in antioxidant defense [52]. This antioxidant system includes a low molecular weight thiol compound, glutathione, GSH, composed of three amino acids:  $\delta$ -glutamyl-cysteinyl-glycine, in which the thiol on the cysteine plays an important role in maintaining the cellular redox state under oxidative stress [53, 54]. An increase in ROS/NOS may induce reversible formation of mixed disulfides between protein sulfhydryl groups (PSH) and glutathione on multiple proteins (*S*-glutathionylation), however, *S*-glutathionylation is an oxidative post-translational modification (PTM) that occurs also on some protein cysteines under basal conditions [53, 55].

Nowadays *S*-glutathionylation is considered a regulatory event in redox signaling and it is involved in physiological processes including kinase signaling, channel function, apoptosis and regulation of transcription [56].

The measurement of glutathionylated proteins by Western blot analysis has emerged as the technique of choice. This approach is possible due to the availability of antibodies that recognize GSH-protein complexes [46, 57].

Also a high performance liquid chromatography (HPLC) procedure can be used for the determination of GSH released from the proteins, an indirect way to determine the extent of protein glutathionylation in a biological system [58].

These two techniques were employed in order to determine the extent of protein glutathionylation in the neurodegeneration cell used in the present study.



### 3. Material and Methods

#### 3.1. Chemicals

Eagle Minimum Essential Medium (EMEM), L-glutamine, non-essential aminoacids, hydrogen ( $H_2O_2$ ) peroxide, dithiothreitol (DTT), *n*-ethylmaleimide (NEM), thiourea, glycerol, sodium pyruvate, sodium azide, formaldehyde and Tween-20®, glycerol, sodium borohydride, *m*-cresol and phenantroline were order from Sigma-Aldrich® (Sintra, Portugal). Opti-Protein XL Marker was from abm® (Richmond, Canada) Penicillin-streptomycin, trypsin and foetal bovine serum (FBS) were order from Gibco® (New York, USA). Triton X-100, sodium dodecyl sulphate (SDS), Ponceau S, trichloroacetic acid and sulfosalicylic acid were order from Merck S.A. (Lisbon, Portugal). Acetic acid and ethanol were order from Panreac S.L.U (Barcelona, Spain). Acrylamide:Bis 29:1, commassie brilliant blue G and phosphoric acid were order from Carl Roth® (Karlsruhe, Germany). Sodium carbonate and urea were from Riedel-de Haën® (Hanover, Germany). DNase I was order from Roche (Basel, Switzerland), and protease inhibitor cocktail EDTA-free were order from Calbiochem® (Massachusetts, USA). Ammonium sulphate was order from Prolabo® (Carnaxide, Portugal) and methanol was from Carlo Erba (Telheiras, Portugal).

Rabbit anti-DNP antibody and Goat Anti-Rabbit IgG HRP conjugated were order from Millipore (Billerica, USA). Mouse anti-GSH antibody was order from Virogen (Watertown, USA), Stabilized Rabbit Anti-mouse HRP conjugated and Goat anti-Rabbit HRP conjugated were from Thermo Fisher Scientific Inc. (Waltham, USA). Rabbit anti-actin antibody was order from Frilabo Lda (Porto, Portugal).

#### 3.2. Plant Material

Commercial blackberry (*Rubus* L. Subgenus *Rubus* Watson) cv. Apache was grown in Fataca Experimental field (Odemira, Portugal) and berries were harvested at full ripeness.

Fruits of a wild blackberry species (*R. vagabundus* Samp.) were collected in September 2009 in Bragança region (northeast region of Portugal) and stored at -80 °C. Fruits were collected from several populations, growing in different locations in order to be representative of species. For this specie, voucher samples were authenticated and deposited at herbarium “João de Carvalho e Vasconcelos”, Instituto Superior de Agronomia, Lisbon, Portugal [23].

#### 3.3. Extract Preparation

The samples were freeze-dried, ground without separation of seeds in an IKA M20 mill to pass a 0.5 mm sieve and stored at -80 °C until further use.

Fruits extracts were prepared using ethanol 50 % (v/v) as previously described [59]. Briefly, to each 1 g of lyophilized powder, 12 mL of ethanol 50 % (v/v) were added and the mixture shaken for 30 min at room temperature in the dark. The extracts obtained were dried under vacuum.

### **3.4. *In vitro* digestion**

Phytochemical alterations during digestion were mimicked using the *in vitro* digestion model (IVD) already described by McDougall *et al.* [15, 60] performed in collaboration with Gordon McDougall and Derek Stewart from The James Hutton Institute, Dundee, Scotland (former Scottish Crop Research Institute). Briefly, the extracts were submitted to conditions that mimic gastric digestion such as adjusted pH to 1.7, addition of pepsin and incubation at 37 °C with shaking at 100 rpm for 2 h. Small intestine conditions were mimicked by addition of pancreatic and bile salts, followed by dialysis with a cellulose tube containing NaHCO<sub>3</sub> to neutralize titratable acidity. After 2 h of incubation at 37 °C, the solution inside the dialysis tubing that mimic the SAF was collected and dried under vacuum.

### **3.5. Cell Culture**

Human neuroblastoma SK-N-MC cells were obtained from the European Collection of Cell Cultures (ECACC) and cultured in EMEM supplemented with 2 mM L-glutamine, 10 % FBS, 1 % (v/v) non-essential aminoacids, 5000 U mL<sup>-1</sup> of penicillin and 5000 µg mL<sup>-1</sup> (w/v) of streptomycin. The cells were maintained at 37 °C in 5 % CO<sub>2</sub> and split at sub confluence of 90-100 %, using 0.05 % trypsin/EDTA. Treatments with digested extracts or with (H<sub>2</sub>O<sub>2</sub>) were carried out in medium with 0.5 % (v/v) FBS. Periods of incubation varied according with the purpose of the experiment.

### **3.6. Time course profile of cells incubated with hydrogen peroxide**

To evaluate a time-dependent response to oxidative stress induction, SK-N-MC cells were incubated with H<sub>2</sub>O<sub>2</sub> for different periods (0-24 h). For that purposes, cells were seeded in T-flasks of 25 cm<sup>2</sup> (1.4 x 10<sup>5</sup> cells mL<sup>-1</sup>). After 24 h, growth medium was removed and cells washed with PBS. Cells were pre-incubated with medium containing 0.5 % (v/v) FBS, and 24 h later, H<sub>2</sub>O<sub>2</sub> at a final concentration of 300 µM was applied with new fresh medium to the T-flask [15].

After incubations periods of 0 h, 1 h, 2 h, 4 h, 6 h, 8 h, and 24 h, cells were collected with trypsin.



### 3.7. Incubation of cells with digested plant extracts

SK-N-MC neuroblastoma cells were incubated for 24 h with digested berries extracts of commercial blackberry (BB) and *R. vagabundus* (RV). Cells were seeded in T-flasks with 25 cm<sup>2</sup> (1.4 x 10<sup>5</sup> cells mL<sup>-1</sup>) and 24 h after seeding, growth medium was removed and cells washed with PBS. Cells were incubated with non-toxic concentration of digested blackberry metabolites: 0.5 µg GAE mL<sup>-1</sup> for, resuspended in medium containing 0.5 % (v/v) FBS [23]. After 24 h of incubation cells were collected with trypsin.

### 3.8. Protein Quantification

Protein quantification was made using modified Lowry's method as reported by Bensadoun and Weinstein [61]. The original method has been modified so that protein can be assayed in the presence of interfering chemicals such as Tris or ammonium sulphate. The absorbance of the samples was measured at 750 nm [61, 62].

### 3.9. Electrophoresis

#### 3.9.1. 1D Electrophoresis

Protein extraction from SK-N-MC samples was performed according to Barata with slightly adjustments [63]. Briefly, protein extracts for detection of protein carbonyls were obtained using a fresh lysis buffer containing 25 mM Tris-HCl at pH 8.0, 1 % (v/v) Triton X-100, 45 % (v/v) ethyleneglycol, 16 mM NEM, 18 mM sodium metabissulfide, 5 mM phenantroline, 1 mg mL<sup>-1</sup> DNase I, 1 % (v/v) cocktail inhibitor proteases III] and 50 mM DTT, whereas protein extracts for detection of glutathionylated proteins were obtained with the same lysis buffer but without DTT. After this, samples were centrifuged at 13,400 g during 10 min at 4 °C and supernatants were collected.

For protein carbonyls detection OxyBlot™ Protein Oxidation Detection kit (Millipore, Billerica, USA) was used. Briefly, the supernatant obtained was immediately used for the derivatization of the carbonyl groups by DNPH. The reaction was stopped by the addition of the neutralization solution from kit, and samples were stored at 4 °C until further use.

For glutathionylated protein, supernatants were collected after centrifugation (13,400 g) and stored with Sample Buffer [1 M (w/v) Tris-HCl, pH 6.8; 1 % (w/v) *m*-cresol purple and 10% (v/v) glycerol] at -20 °C until further use.

Fifteen micrograms of protein were subjected to SDS-PAGE in 10 % (w/v) acrylamide gels with 1 mm thick at 200 V during 1 h. The electrophoresis buffer used was composed by 25 mM (w/v) Tris base, 192 mM (w/v) glycine and 0.1 % (w/v) SDS [64]. Protein standards were run along with the sample.

### 3.9.2. 2D Electrophoresis

Protein extraction from SK-N-MC samples was performed according to Esteves, S. [65]. Briefly, cells were trypsinized and centrifuged at 200 g during 10 min. The cells were washed with PBS, and centrifuged at 200 g during 10 min. Then the supernatant was discarded and a resuspension buffer [60 mM DTT, 7 M Urea, 2 M Thiourea, 4 % (w/v) CHAPS, 0.4 % (v/v) Triton X-100, 2 % (v/v) IPG Buffer (1:2, 3-10NL:4-7L), 1 mg mL<sup>-1</sup> DNase, 1 % (v/v) cocktail inhibitor proteases III] was added to the cells. Protein samples were collected after centrifugation at 13,400 g during 10 min and stored at -20 °C until further use.

For isoelectric focusing electrophoresis (IEF), the IPGphor system was used (Amersham Biosciences, Uppsala, Sweden) with a non-linear gradient gel of pH 3-10, 13 cm (IPGstrips, GE Healthcare, Uppsala, Sweden).

The samples, containing 65 µg of protein were centrifuged at 13,400 g at room temperature during 5 min, and the supernatant was applied to the Strip Holder. The IEF was carried out at 30 V for 12 h, followed by 250 V for 1 h, 500 V for 1.5 h, 1000 V for 1.5 h, 2500 V for 1.5 h, 8000 V for 1 h gradient and 8000 V for 4 h at 20 °C. In the end of the IEF the strips were stored at -20 °C until second dimension separation was performed [65].

Prior to SDS-PAGE the IPGstrips were equilibrated twice for 15 min in a buffer solution containing 50 mM Tris-HCl (pH 6.8), 6 M urea, 1 % (w/v) SDS, and 30 % (v/v) glycerol. DTT in a concentration of 0.06 (w/v) mM was added to the first equilibration step and 0.135 mM (w/v) iodoacetamide to the second one. The samples were subjected to SDS-PAGE in 12.5% (v/v) acrylamide gels with 1 mm thick. The electrophoresis buffer used was composed by 25 mM Tris base (w/v), 192 mM (w/v) glycine, 0.1 % (w/v) SDS [64]. Protein standards were run along with the sample using 15 mA per gel for 15 min and then 30 mA per gel for 3 h.

### 3.9.3. Gel Staining

#### 3.9.3.1. Commassie Brilliant Blue

This staining was done according to Neuheff *et al.* [66]. After second dimension, the gels were fixed in a solution containing 2 % (v/v) of phosphoric acid and 50 % (v/v) of methanol during 2 h, followed by 3 wash steps with bidistilled of 20 min each. Then the gels were incubated in 34 % (v/v) methanol, 17 % (w/v) ammonium sulphate and 2 % (v/v) of phosphoric acid during 1 h. After this period, a solution containing 1.1 % (w/v) Commassie Brilliant Blue G and 34 % (v/v) methanol was added and gels stayed in this solution for 2 days. Gel images were acquired by the Image Scanner (Amersham Biosciences, Uppsala, Sweden).

#### 3.9.4. 2DE Gel analysis

Commassie Brilliant Blue stained gels were used for image analysis.

Gel images were analysed in Progenesis SameSpots software (Nonlinear Dynamics, Newcastle, United Kingdom) for spot detection, measurement and matching.

The first step in the analysis of Progenesis SameSpots software was image control. Images went through a process of image quality assessment for accurate image analysis.

Second, an appropriate reference image was selected to align the images to and then the areas of the gel to be excluded from the analysis were defined. Once made the detection of spots they were edited, validated and reviewed.

One of the crucial steps in this analysis is spot volume normalisation: the intensity of each spot in a gel is expressed as a proportion of the total protein intensity detected in the entire gel [67, 68].

Individual spots with irregularities (*i.e.* ink spikes) were rejected and a protein spot was kept for further analysis and declared reliable if at least  $n-1$  normalized volume values were available in each condition.

#### 3.10. Mass spectrometry analysis

After protein spots excision from the 2DE gels, the protein spots were submitted to a digestion with trypsin. After this, the trypsin digested proteins were analyzed by matrix-assisted laser desorption/ionization/time-of-flight (MALDI-TOF/TOF) performed in collaboration with Proteomics Unit by the INIBIC- University Hospital Complex of Coruña.

Briefly, protein spots were diced in small pieces and in-gel digested following standard procedures [69]. The samples were desiccated with acetonitrile, reduced with DTT, alkylated with iodoacetamide and trypsin-digested ( $6 \text{ ng } \mu\text{L}^{-1}$ , Roche (Basel, Switzerland)) for 16 h at 37 °C. Peptides were then extracted, dried in a speed-vac reconstituted in 0.1 % trifluoroacetic acid and de-salted using nu-tipC18 (Glygen).

The samples were analyzed in a MALDI-TOF/TOF instrument (4800 ABSciex) and 4000 series Explorer v.4.2 software was used to generate the spectra and peak list. MS acquisitions were done with a laser voltage of 3800 kV and 1500 shots/spectrum. Automated precursor selection was done using an interpretation method (up to 20 precursors/fraction, Signal to Noise lower threshold = 50) with a laser voltage of 4800 and 1500 shots/spectrum. Collision-induced dissociation (CID) collision energy range: medium.

Fragmentation spectra were acquired by selecting the 20 most abundant ions of each MALDI-TOF peptide mass map (excluding trypsin autolytic peptides and other background ions) and

averaging 2000 laser shots per fragmentation spectrum. The parameters used to analyze the data were a signal-to-noise threshold of 20, minimum area of 100 and a resolution higher than 10, 000 with a mass accuracy of 20 ppm. For database queries and protein identification, the monoisotopic peptide mass fingerprinting data obtained from MS and the amino acid sequence tag obtained from each peptide fragmentation in MS/MS analyses were used to search for protein candidates using Mascot v.1.9 from Matrix Science ([www.matrixscience.com](http://www.matrixscience.com)). Peak intensity was used to select up to 50 peaks per spot for peptide mass fingerprinting and 50 peaks per precursor for MS/MS identification. Tryptic autolytic fragment-, keratin-, and matrix-derived peaks were removed from the data set utilized for database search. The search for peptides mass fingerprints and tandem MS spectra were performed in NCBIInr database (August 2012). Fixed and variable modifications were considered (Cys as S-carbamidomethyl and Met as oxidized methionine, respectively), allowing one trypsin missed cleavage. MS/MS ions search were conducted with a mass tolerance of 50 ppm on the parent and 0.3 Da on fragments. Decoy search was done automatically by Mascot on randomized database of equal composition and size. Mascot scores for all protein identifications were higher than the accepted threshold for significance (at the  $p < 0.050$  level, positive rate measured to be 0.047).

### **3.11. Western Blot**

#### **3.11.1. Electrotransfer of polypeptides**

The electrotransfer of polypeptides was done according to Swerdlow *et al.* [70]. After SDS-PAGE, gels were incubated in electrotransfer buffer containing 25 mM (w/v) Tris base, 19 mM (w/v) glycine, 0.1 % (w/v) SDS and 20 % (v/v) of methanol at pH 8.3 during 15 min. PVDF membranes (Amersham Biosciences, Uppsala, Sweden) were incubated in methanol followed by incubation in electrotransfer buffer. The gel and the membrane were assembled in the transfer cell (Trans-Blot electrophoretic transfer cell, BioRad, Amadora, Portugal) containing transfer buffer. Transfer was carried out at 70 V for 1.5 h for gels with 1 mm thick at 4 °C.

#### **3.11.2. Ponceau S Staining**

Ponceau S staining solution [0.2 % (w/v) Ponceau S, 3 % (w/v) trichloroacetic acid, 3 % (w/v) sulfosalicylic acid] was used for the detection of proteins on PVDF membranes.

After electrophoresis, the blotted membrane was immersing in Ponceau S staining solution during 5 to 10 min, and then washed with bi-distilled water until the appearance of polypeptides, according to manufactures instruction (Merck S.A. Lisbon, Portugal).

### 3.11.3. Immunodetection

OxyBlot™ Protein Oxidation Detection kit (Millipore, Billerica, USA) was used according to the manufacturer's instructions for the detection of carbonylated proteins, and the detection of glutathionylated proteins was done according to Newman *et al.* [54] with slightly adjustments.

After protein transfer or Ponceau S staining, membranes were dried at room temperature and blocked with 5 % (w/v) membrane blocking agent (MBA-GE Healthcare, Uppsala, Sweden) in PBS containing 0.01 % (w/v) sodium azide and 0.1 % (v/v) Tween 20® (PBS-Tween) overnight at 4 °C or 1 h at room temperature.

The membranes were incubated with primary antibody in blocking/dilution buffer for 2 h, which was verified to develop better signal than one hour of incubation, with gentle stirring at room temperature. The membranes were then washed twice for 5 min with PBS-Tween and once for 15 min with PBS-Tween followed by incubation with secondary antibody in blocking/dilution buffer for 1 h at room temperature. The conditions for each antibody are described in Table 3.1. Antibody detection was performed with the chemiluminescent substrate (FemtoMax Super Sensitive Chemiluminescent HRP Substrate; Rockland Inc., Gilbertsville, USA). Membrane images were acquired in the Molecular Imager ChemiDoc XRS (Quantity One© software v. 4.6.6; BioRad, Amadora, Portugal).

**Table 3.1** - Antibodies and dilutions used in Western blot analyses.

	<b>Protein Carbonyls</b>	<b>Glutathionylated Proteins</b>	<b>Loading Control</b>
<b>1° Antibody</b>	Rabbit anti-DNP antibody (1:150)	Mouse anti-GSH antibody (1:1000)	Rabbit anti-actin antibody (1:1000)
<b>2° Antibody</b>	Goat Anti-Rabbit IgG HRP conjugated (1:300)	Stabilized Rabbit Anti-mouse HRP conjugated (1:2500)	Goat anti-Rabbit HRP conjugated (1:50000)

### 3.12. **Measurement of glutathione released from glutathionylated proteins**

This method was performed in collaboration with Dr Inês Figueira from DSB Lab.

To quantify GSH and GSSG, cold 10 % (w/v) metaphosphoric acid was carefully added to samples or standards. After incubation (4 °C, 10 min) and centrifugation (16,000 g, 20 min, 4 °C) supernatants were collected (50 µL for determination of GSH and 200 µL for determination of GSSG).

The procedure for the reduction of proteins by sodium borohydride was performed according to Hiil, *et al.* [57]. The pellet (PSSG – Protein S-glutathionylated) was washed 4 times with cold 10 % (w/v) metaphosphoric acid, sonicated and then samples were centrifuged (1,000 g, 5 min, 4 °C). After this 0.25% (w/v) sodium borohydride in 10 mM (w/v) Tris-HCl, pH 7.5, was added to the samples (45 min at 41 °C). The next step was acidification of the samples by adding cold 10 % (w/v) metaphosphoric acid. After incubation (4 °C, 10 min) and centrifugation (16,000 g, 20 min, 4 °C), supernatants were collected (50 µL for determination of GSH and 200 µL for determination of GSSG).

Derivatization was performed accordingly to Kand'ar and co-workers [71], that was adapted from Hissin and Hilf [72]. Briefly, for GSH analysis 1 mL of 0.1 % (w/v) EDTA in 0.1 M sodium hydrogen phosphate, at pH 8.0, was added to 50 µL of supernatant. To 20 µL portion of this mixture, 300 µL of 0.1 % (w/v) EDTA in 0.1 M PBS, at pH 8.0, and 20 µL of 0.1 % (w/v) OPA in methanol, were added. Tubes were incubated at 25 °C for 15 min in the dark. The reaction mixture was then stored at 4 °C until analysis.

For GSSG analysis, 200 µL of supernatant was incubated at 25 °C with 200 µL of 40 mM NEM for 25 min in dark. To this mixture, 750 µL of 0.1 M NaOH was added. A 20 µL portion was taken and mixed with 300 µL of 0.1 M NaOH and 20 µL of 0.1 % OPA. Tubes were incubated at 25 °C for 15 min in dark and stored at 4 °C until analysis. Chromatographic analysis was accomplished using isocratic elution on C18 analytical column (Supelcosil™ ABZ+Plus HPLC Column 15 cm x 4.6 mm, 3 µm (Supelco)) at 40 °C on an Acquity™ Ultra Performance LC system (Waters). The mobile phase consisted of 15 % (v/v) methanol in 25 mM (v/v) PBS at pH 6.0. The flow rate was kept constant at 0.7 mL min<sup>-1</sup>. The excitation and emission wavelengths were set at 350 and 420 nm, respectively. The amount of GSH and GSSG was quantified from the corresponding peak area using Empower® Pro 2.0 software. The concentration of GSH and GSSG in the samples was determined from standard curves with ranges 0-100 µM for GSH and 0-5 µM for GSSG. Values were normalized for total protein content.

### 3.13. Statistical Analysis

A complete data matrix of protein spot normalized volumes was generated by replacing the missing values in a condition by the mean of existing values for that protein spot [73]. The protein spots were statistically evaluated by ANOVA-Tukay HSD (Analysis of variance-Honest Significant Difference) test when normality test passed, however, when normality test failed, One Way ANOVA on Ranks was used.

For all the statistical analysis performed the SigmaStat v.3.10 software (Systat software Inc, Erkrath, Germany) was used.





## 4. Results and Discussion

### 4.1. Evaluation of Oxidative Stress

To mimic pathological situations with increased oxidative stress, peroxides are often used to implement cell models [74]. To reproduce a neurodegeneration cell model, 300  $\mu\text{M}$   $\text{H}_2\text{O}_2$  was used to induce oxidative stress in SK-N-MC neuroblastoma cells, a concentration of  $\text{H}_2\text{O}_2$  that reduces cells viability to approximately 50 % after 24 h of incubation [15].

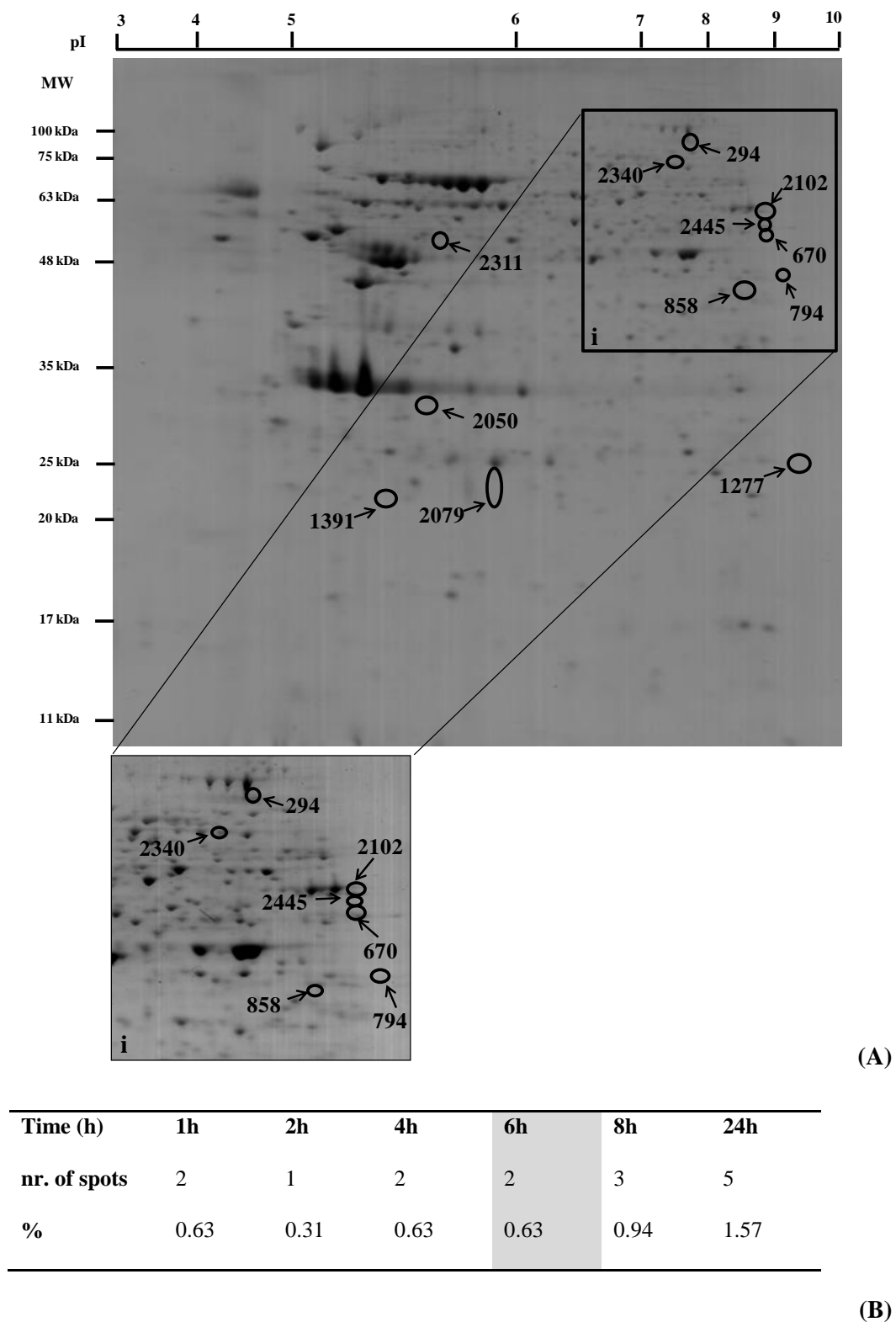
#### 4.1.1. Time course profile of protein extracts from SK-N-MC cells treated with hydrogen peroxide

To detect the proteins altered during oxidative stress in neuronal cells, the cells were treated with 300  $\mu\text{M}$  of  $\text{H}_2\text{O}_2$  for 1 h, 2 h, 4 h, 6 h, 8 h and 24 h. After protein extraction, the proteins were separated using 2DE technique. The separated proteins were visualized with CBB and analyzed with Progenesis SameSpots software.

After statistical analysis, 318 protein spots were pinpointed, from which 12 were statistical different from the control which corresponds to 3,77 % of the total protein spots (Fig. 4.1 (A)). For 1 h, 2 h, 4 h, 8 h and 24 h of stress injury the protein spots altered were upregulated, however, after 6 h of stress the protein spots were downregulated relatively to control (Fig. 4.1 (B)); the time course profile for each protein spot as well as the estimated pI and MW (kDa) are described in Table 4.1.

Exposure of cells to  $\text{H}_2\text{O}_2$  for 24 h caused more alterations in the protein pattern than in the remaining treatments, while 2 h of incubation with  $\text{H}_2\text{O}_2$  had less effect on protein pattern. These results showed that longer exposure times to  $\text{H}_2\text{O}_2$  lead to more changes in the pattern of the proteins (Fig. 4.1 (B)).

The identification by MS of the protein spots statistically different is currently an ongoing work.



**Fig. 4.1** - **(A)** Representative 2DE control gel of SK-N-MC cells (65 µg). The gel was CBB stained. Twelve spots were found to change quantitatively between the control and stress conditions evaluated (0-24 h), and numbered spots have been sent for protein identification by MS; **(i)** Zoom in of some protein spots of 2DE gel with high contrast; **(B)** Comparison of protein spots differentially expressed against control, white columns for upregulated proteins and gray column for downregulated protein spots.

**Table 4.1** - Time course profile for the expression of protein spots differentially expressed in SK-N-MC cells treated with 300  $\mu$ M H<sub>2</sub>O<sub>2</sub> and their characteristics (pI and MW (kDa)). Differences between treatments in relation to control are denoted as \*p<0.05 \*\*p<0.01, \*\*\*p<0.001.

Time course profile and normalized volumes	pI	MW (kDa)
<p><b>294</b></p> <p>Normalized volume (x10<sup>6</sup>)</p> <p>Time (h)</p>	7.9	80.2
<p><b>2340</b></p> <p>Normalized volume (x10<sup>6</sup>)</p> <p>Time (h)</p>	7.2	74.1
<p><b>2102</b></p> <p>Normalized volume (x10<sup>6</sup>)</p> <p>Time (h)</p>	8.6	63.9

Time course profile and normalized volumes	pI	MW (kDa)
<p><b>2445</b></p> <p>Normalized volume (<math>\times 10^6</math>)</p> <p>Time (h)</p>	8.6	60.5
<p><b>2311</b></p> <p>Normalized volume (<math>\times 10^6</math>)</p> <p>Time (h)</p>	5.6	57.9
<p><b>670</b></p> <p>Normalized volume (<math>\times 10^6</math>)</p> <p>Time (h)</p>	8.6	57.7

Time course profile and normalized volumes	pI	MW (kDa)																
<div><p><b>794</b></p><p>Normalized volume (x10<sup>6</sup>)</p><p>Time (h)</p><table><caption>Data for pI 794</caption><thead><tr><th>Time (h)</th><th>Normalized volume (x10<sup>6</sup>)</th></tr></thead><tbody><tr><td>0</td><td>0.7</td></tr><tr><td>1</td><td>0.8</td></tr><tr><td>2</td><td>0.9</td></tr><tr><td>4</td><td>1.0</td></tr><tr><td>6</td><td>0.9</td></tr><tr><td>8</td><td>1.2</td></tr><tr><td>24</td><td>2.1*</td></tr></tbody></table></div>	Time (h)	Normalized volume (x10 <sup>6</sup> )	0	0.7	1	0.8	2	0.9	4	1.0	6	0.9	8	1.2	24	2.1*	9.2	49.7
Time (h)	Normalized volume (x10 <sup>6</sup> )																	
0	0.7																	
1	0.8																	
2	0.9																	
4	1.0																	
6	0.9																	
8	1.2																	
24	2.1*																	
<div><p><b>858</b></p><p>Normalized volume (x10<sup>6</sup>)</p><p>Time (h)</p><table><caption>Data for pI 858</caption><thead><tr><th>Time (h)</th><th>Normalized volume (x10<sup>6</sup>)</th></tr></thead><tbody><tr><td>0</td><td>2.1</td></tr><tr><td>1</td><td>3.5***</td></tr><tr><td>2</td><td>1.4</td></tr><tr><td>4</td><td>2.5</td></tr><tr><td>6</td><td>2.6</td></tr><tr><td>8</td><td>2.4</td></tr><tr><td>24</td><td>2.6</td></tr></tbody></table></div>	Time (h)	Normalized volume (x10 <sup>6</sup> )	0	2.1	1	3.5***	2	1.4	4	2.5	6	2.6	8	2.4	24	2.6	8.2	47.0
Time (h)	Normalized volume (x10 <sup>6</sup> )																	
0	2.1																	
1	3.5***																	
2	1.4																	
4	2.5																	
6	2.6																	
8	2.4																	
24	2.6																	
<div><p><b>2050</b></p><p>Normalized volume (x10<sup>6</sup>)</p><p>Time (h)</p><table><caption>Data for pI 2050</caption><thead><tr><th>Time (h)</th><th>Normalized volume (x10<sup>6</sup>)</th></tr></thead><tbody><tr><td>0</td><td>5.0</td></tr><tr><td>1</td><td>7.0</td></tr><tr><td>2</td><td>11.0</td></tr><tr><td>4</td><td>7.0</td></tr><tr><td>6</td><td>11.0</td></tr><tr><td>8</td><td>25.0***</td></tr><tr><td>24</td><td>10.0</td></tr></tbody></table></div>	Time (h)	Normalized volume (x10 <sup>6</sup> )	0	5.0	1	7.0	2	11.0	4	7.0	6	11.0	8	25.0***	24	10.0	5.7	32.0
Time (h)	Normalized volume (x10 <sup>6</sup> )																	
0	5.0																	
1	7.0																	
2	11.0																	
4	7.0																	
6	11.0																	
8	25.0***																	
24	10.0																	

Time course profile and normalized volumes	pI	MW (kDa)
<p><b>1277</b></p> <p>Normalized volume (x10<sup>6</sup>)</p> <p>Time (h)</p>	9.5	26.1
<p><b>2079</b></p> <p>Normalized volume (x10<sup>6</sup>)</p> <p>Time (h)</p>	5.9	24.2
<p><b>1391</b></p> <p>Normalized volume (x10<sup>6</sup>)</p> <p>Time (h)</p>	5.4	23.5

Taking into account what is already known about the induction of stress in this cell model (50% reduction in cell viability, changing on free GSH levels and caspases activity) it would be expectable that the percentage of protein spots that are different expressed from control would be higher than the obtained [23]. However, these facts could indicate that protein changes do not occur in the most abundant proteins, those which can be detect on global proteome analysis, but most likely occur in the less abundant proteins, specific sub proteomes or specific proteins.

The 2DE technique exhibit a great potential to resolve thousands of proteins simultaneously, providing important clues even for PTM's that involve changes in protein total charge, but has several limitations like the inability to detect low-abundance proteins, this become a limiting step because these proteins can be hampered by protein with similar size and charge or by expression levels below the current detection limits of the technique used [4, 36, 38]. Current available proteomic approaches are estimated to focus on 30 % most abundant proteins such as cytoskeleton proteins that tend to interfere with proteomic analysis by masking proteins with lower copy numbers. An advantage of selecting protein populations for proteomic analysis is that it substantially decreases the complexity of extracts and thus increases the likelihood of identifying proteins with lower abundance [36].

It becomes clear that could be interesting to fractionate our sample; this allows to reduce the complexity of protein/peptide mixtures and to separate various groups of proteins for subsequent analysis [75].

Proteome analysis was the first approach but since oxidative reactions are the main features during neurodegeneration we looked more specifically for redox proteomics alterations, focusing in some redox alterations in particular some chemical groups in the proteins, such as protein carbonyls and protein glutathionylation.

#### 4.1.2. Protein Carbonyls

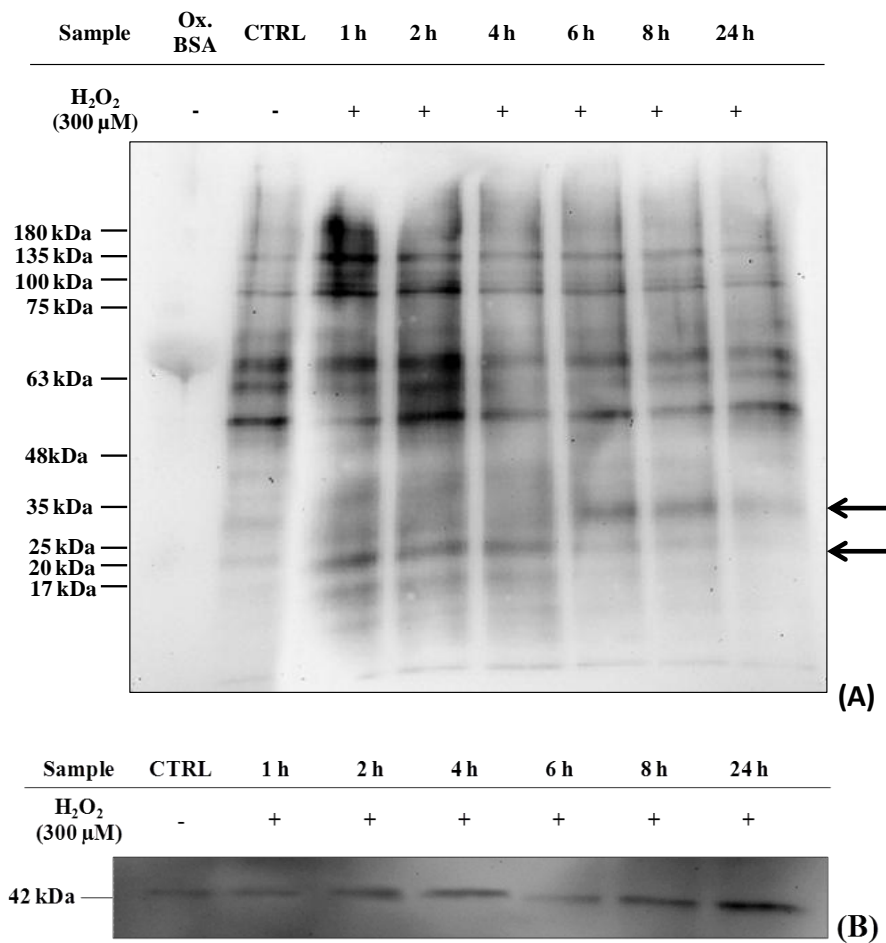
The determination of carbonyl groups has been widely employed as a parameter of protein oxidation to characterize tissue alterations occurring in neurodegenerative diseases [76].

Protein carbonyls can be easily detected by forming a hydrazone derivative with DNPH. This product can then be detected by various methods such as spectrophotometric assay, enzyme-linked immunoabsorbent assay (ELISA), and 1DE or 2DE followed by Western blot immunoassay [50, 77].

The detection of oxidatively modified proteins by immunoblotting has advantages over the methods listed above: i) the sensitivity of the method is at least 100 times greater than those obtained by other procedures; ii) individual oxidized proteins can be separated and identified from a complex mixture by 1DE/2DE; and the oxidative status of each polypeptide can be analyzed quantitatively by comparison of the signal intensity of the same polypeptide in different lanes on the same gel. Based on this we decided to use this method to determine carbonylated proteins.

In our work, SK-N-MC samples were tested by the immunodetection in membrane of the adduct protein-hydrazone after resolve in SDS-PAGE, by using the OxyBlot™ Protein Oxidation Detection kit. In parallel, also a positive control (oxidized BSA) was derivatized and analyzed.

After some adjustments in the protocol to achieve better results as described in section 3, the pattern of carbonylated proteins obtained for SK-N-MC cells treated with H<sub>2</sub>O<sub>2</sub> was evaluated (Fig 4.2). Slightly differences for polypeptides with MW between 35 and 17 kDa were detected. Apparently the first two hours of stress promote an overall increase in the signal of carbonylated protein (Fig 4.2 (A)).



**Fig. 4.2 - (A)** Protein carbonyl profile of SK-N-MC cells submitted to oxidative injury (300 μM H<sub>2</sub>O<sub>2</sub>) with different times of exposure (0-24 h), in comparison to control (CTRL), as well as oxidized BSA (Ox. BSA – positive control); **(B)** immunodetection of the loading control (β-actin). Protein carbonyl profile was obtained after sample derivatization using OxyBlot™ Protein Oxidation Detection kit (Intergen) Western blot was exposed to chemiluminescence detection using FemtoMax Super Sensitive Chemiluminescent HRP Substrate – Rockland Inc. A representative image is shown;

A polypeptide of ~30 kDa appears with increase oxidation only for incubations longer than 6 h. On the other hand an early response is observed for a polypeptide with lower MW (~20 kDa), with oxidation trough carbonylation in the first 4 h of stress returning to the control levels after this period.



These different responses to stress over the time in the oxidation state of proteins suggests that cells metabolism produces different responses to early and late oxidative injury. Further studies to identify the polypeptides differentially altered will be helpful to understand the mechanisms involved in this stress response and potential protein targets to observe after cytoprotection by the digested berries extracts.

Differences in polypeptide intensity are not due to different amounts of protein loaded into the gel, but with greater expression of these polypeptides for the respective conditions, since there are no significant differences in the loading control (Fig. 4.2 (B)).

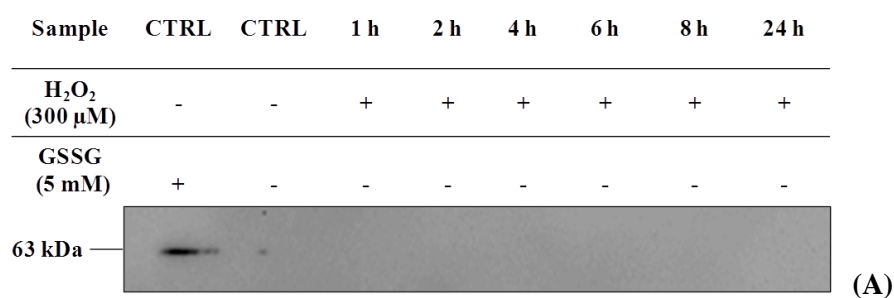
The ability to visualize proteins on high resolution 2DE immunoblots offers significant advantages over 1DE molecular weight separation, so in future work we will also try to implement 2DE immunoblots for the detection of carbonylated proteins [77].

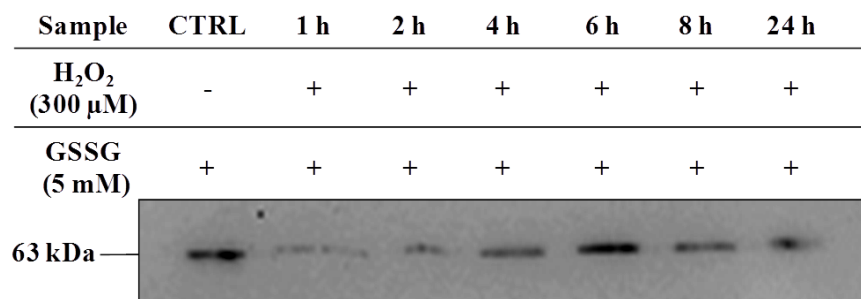
#### 4.1.3. Protein S-Glutathionylation

Over the years methods for measuring glutathionylated proteins were developed to quantify the total amount of GSH bound to proteins. These approaches demonstrated that GSH forms covalent bonds with proteins and that the levels of glutathionylated proteins (or mixed disulfides) change with specific diseases or pathological conditions associated with oxidative stress [57].

Complementary approaches were subject to consideration in this work: an immunological method and a high performance liquid chromatography (HPLC). In our work, SK-N-MC protein samples were assayed by immunodetection in a PVDF membrane after SDS-PAGE. In parallel a positive control (cells from control + 5 mM GSSG) was analyzed.

The pattern of glutathionylated proteins obtained for SK-N-MC cells treated with  $H_2O_2$  showed that only the positive control presents a glutathionylated protein, for the remaining incubation times with  $H_2O_2$  no polypeptide appears glutathionylated. (Fig. 4.3 (A)).





(B)

**Fig. 4.3** - Protein glutathionylation profile of SK-N-MC cells submitted to oxidative injury (300 μM H<sub>2</sub>O<sub>2</sub>) with different times of exposure (0-24 h), in comparison to (A) control (CTRL), as well as (B) oxidized samples with 5 mM GSSG. Glutathionylated protein profile was obtained after incubation with mouse anti-GSH antibody (Virogen). Western blot was exposed to chemiluminescence detection using FemtoMax Super Sensitive Chemiluminescent HRP Substrate – Rockland Inc. A representative image is shown;

An indirect way to evaluate which proteins from our model are prone to be glutathionylated and assess if stress affects that ability is to add 5 mM of GSSG to the protein samples. The Fig. 4.3 (B) shows that a polypeptide with ~63 kDa has avidity to be glutathionylated; interestingly, we observed that this pattern ability to be glutathionylated increases after 4 h of stress. Previous results from DSB Lab (see annexes, Fig. S1) showed that GSH levels start to decrease after 4 h of H<sub>2</sub>O<sub>2</sub> incubation, this decrease is consistent with the glutathionylation avidity increase detected (Fig. 4.3 (B)). Further studies should be done to identify this polypeptide.

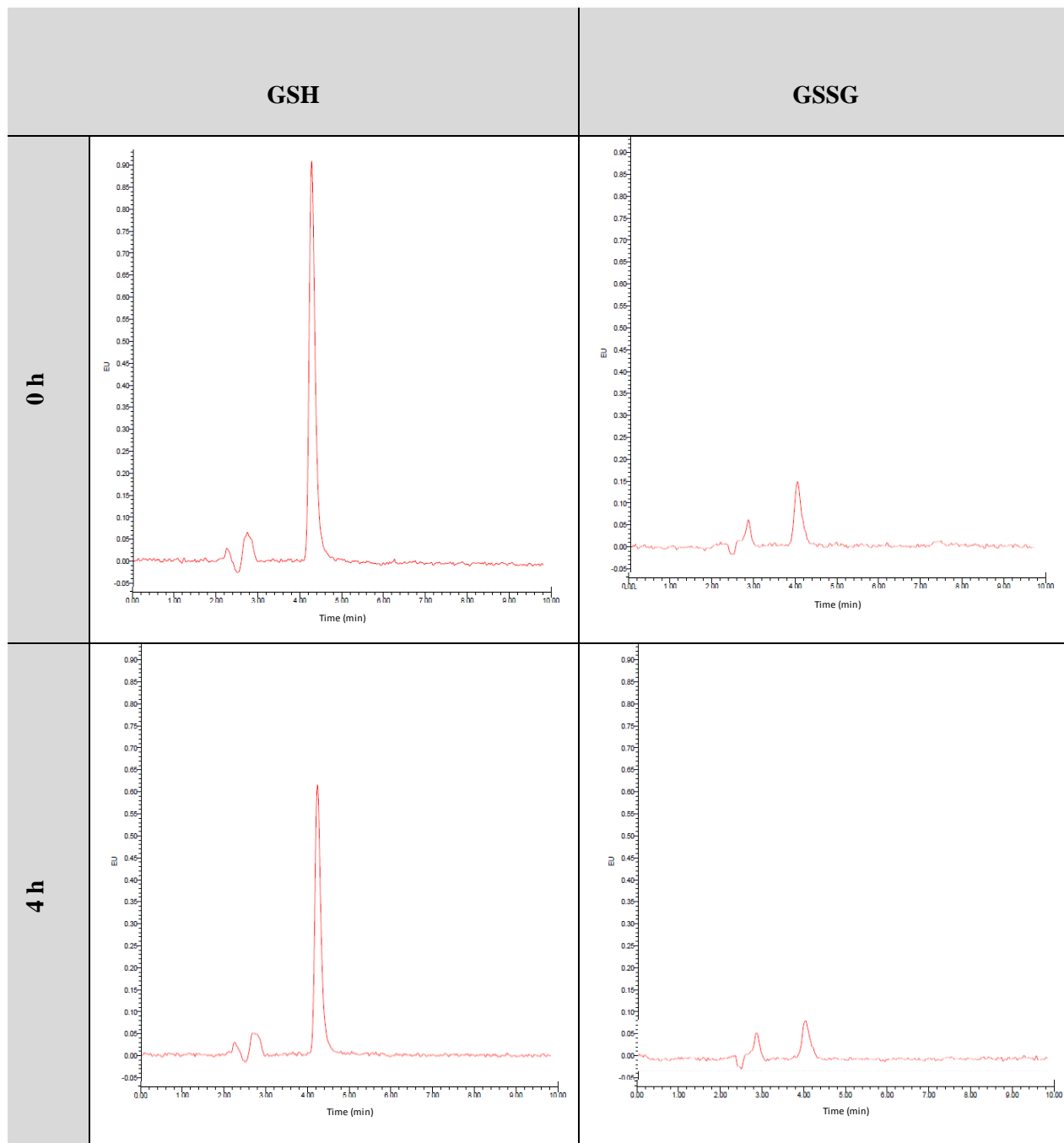
The other approach used to detect and quantify GSH released from glutathionylated proteins was HPLC technique. Protein-GSH complexes can be reduced by sodium borohydride, and the thiol liberated measured by HPLC [78].

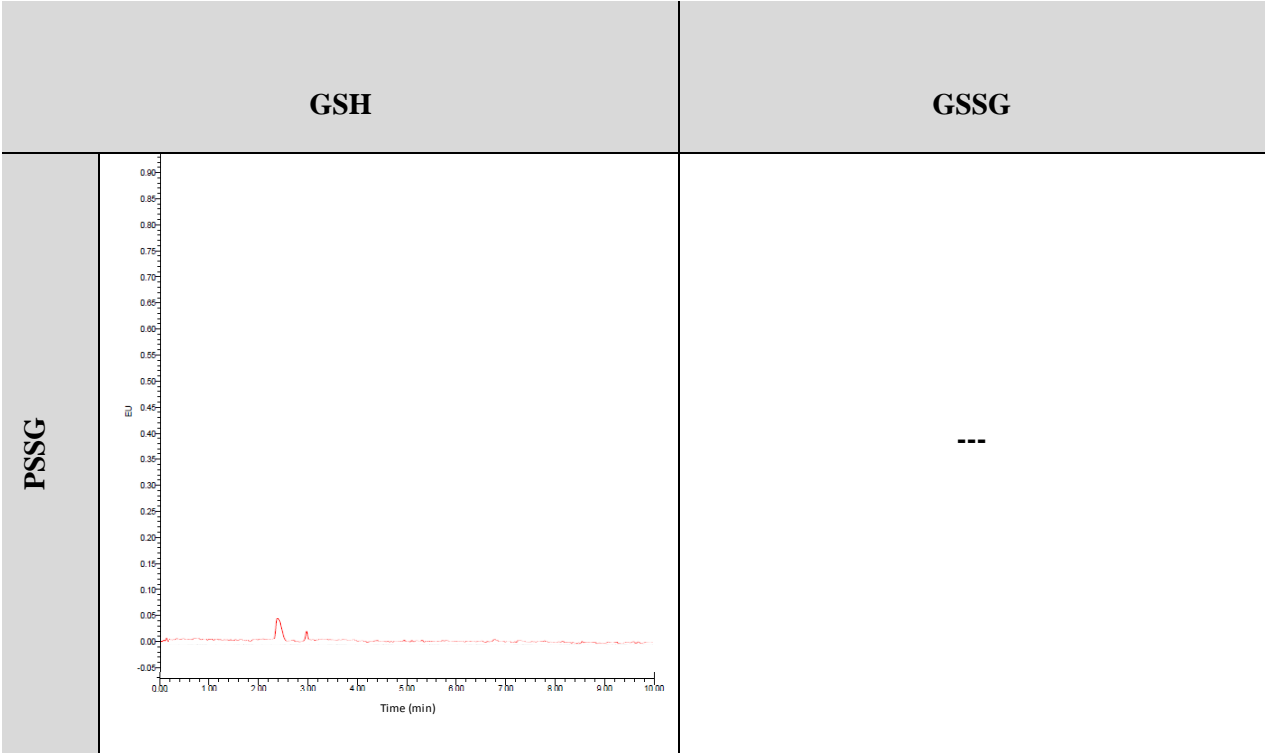
The detection is based in the fact that both reduced and oxidized forms of glutathione (GSH/GSSG) form a stable, highly fluorescent tricyclic derivate with OPA [71, 72]. This method overcomes most of the difficulties of enzymatic and chemical procedures, increasing the detection power relatively to spectrophotometric or fluorimetric methods once it is a chromatographic approach [72].

Cells were incubated with H<sub>2</sub>O<sub>2</sub> during 4 h, this time was chosen accordingly with data from GSH levels since oxidative stress conditions lead to GSH oxidation (see annexes Fig. S1). A decrease of free GSH inside the cell is observed after 4-6 h of treatment. Since there is no increase in GSSG content (data not shown), we may expect that GSH may be used for other cellular mechanisms, namely *S*-glutathionylation.

The results from HPLC analysis (Table 4.2) showed that there was not GSH liberated from proteins, compared with free GSH from control and 4 h of incubation, *i.e.*, these results agree with those obtained previously by Western blot analysis, there was no glutathionylated protein.

**Table 4.2** - HPLC chromatograms of GSH and GSSG for SK-N-MC cells incubated with H<sub>2</sub>O<sub>2</sub> (300 µM) during 4 h and HPLC chromatograms for GSH released from glutathionylated proteins (PSSG) relatively to SK-N-MC control cells (0 h). Glutathione-OPA adduct was monitored at excitation and emission wavelengths of 350 and 420 nm, respectively.





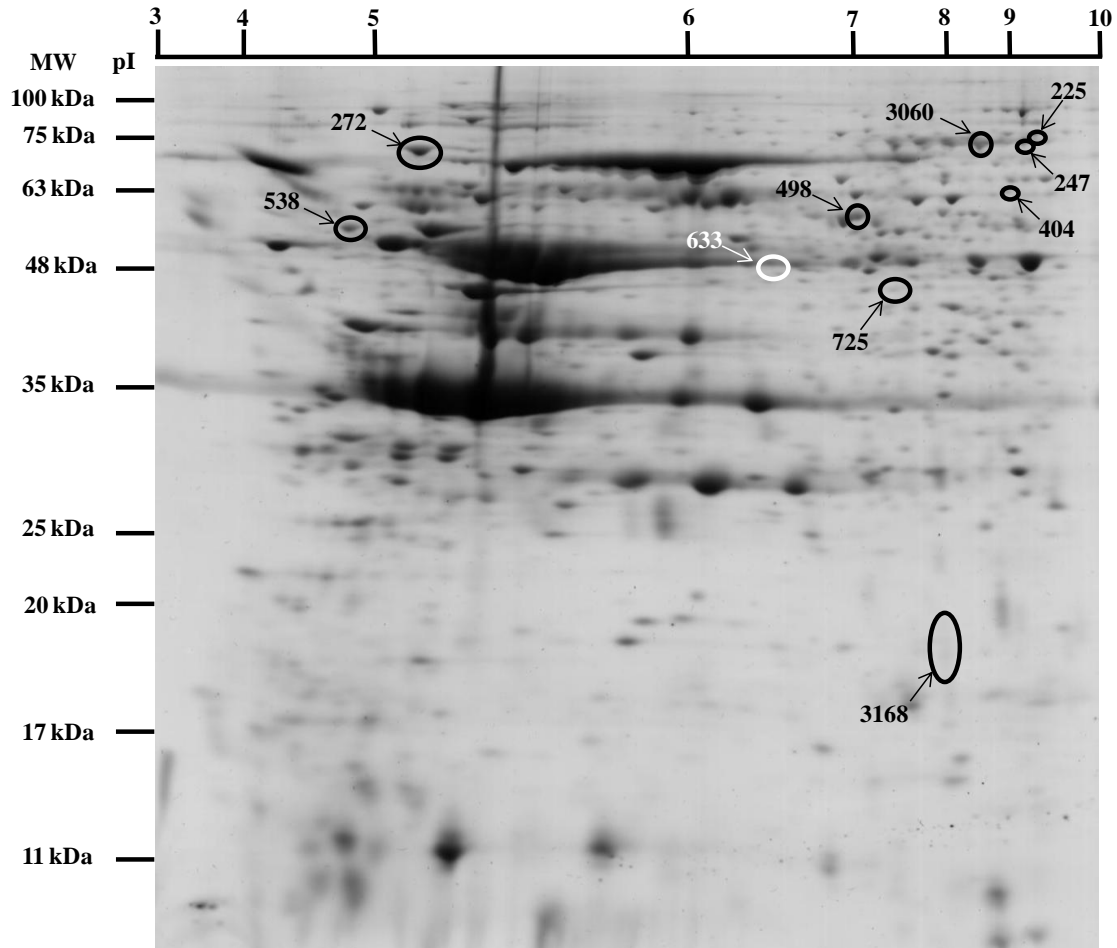
These results can be explained by the fact that *S*-glutathionylation is a reversible PTM and the amount of cells used in the experiment was too small to determine GSH levels. To overcome this limiting step, in further studies we should use purification methods, such as the purification of glutathionylated proteins on a GSH-affinity column before Western blot and HPLC analyses to improve our results [57, 79].

**4.2. Protein pattern of SK-N-MC cell line treated with different digested berry extracts**

Recent studies in DSB Lab evaluate the potential of digested blackberries (commercial blackberry and *R. vagabundus*) as dietary strategies to prevent or retard neurodegeneration. The results demonstrated that digested berry extracts were able to maintain cell membrane integrity, protecting neurons from death, and that the differences on cell protection mediated by BB and RV was accompanied by caspases -3 and -7 activation and a differential modulation of GSH levels [15, 23].

The use of *in vitro* digested extracts of berries is very important since it mimics the metabolites that may reach the external surface of the blood brain barrier (BBB) and then could induce some neuroprotective effects. Also the levels tested are in the range of the levels detected in the serum of human organism which ensures to mimic physiological conditions [15]. Based on this, in

order to contribute to the understanding of the mechanisms underlying these beneficial effects a proteomic analysis was used. The results are shown in Fig. 4.4.



**Fig. 4.4** - Representative 2DE control gel of SK-N-MC cells. The gel was CBB stained. One protein spot (white spot) from SK-N-MC cells incubated with *R. vagabundus* (RV) during 24 h, and 9 protein spots (black spots) from SK-N-MC cells incubated with commercial blackberry (BB) during 24 h were statistical different from control. Numbered spots were sent for protein identification by MS.

From the statistical analysis of 277 protein spots only 1 protein spot (white spot) from SK-N-MC cells incubated with RV was statistically different from control, and 9 protein spots (black spots) from SK-N-MC cells incubated with BB were statistically different from control.

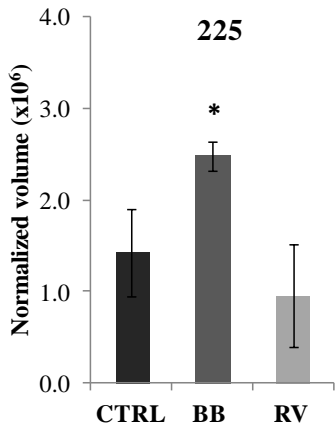
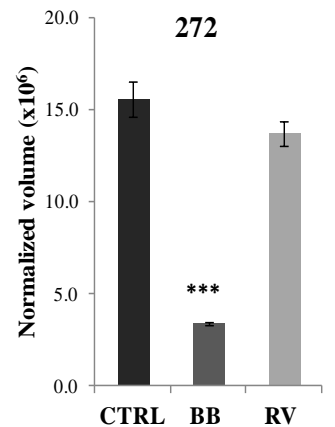
The results also showed that the majority of the statistically different spots are protein spots with MW more than 40 kDa and with basic pI (Fig. 4.4).

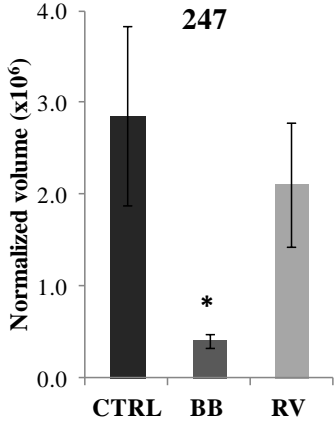
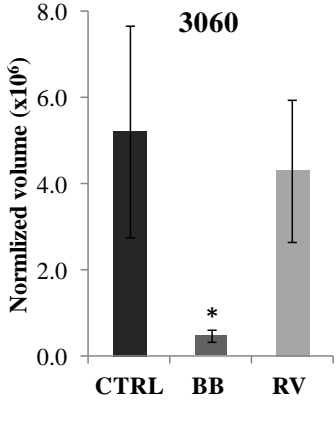
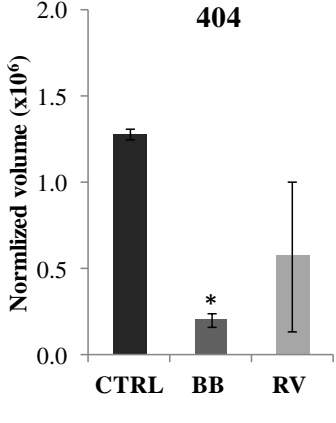
When SK-N-MC cells were incubated with digested berries extracts, the number of altered protein spots was higher for BB than for RV. These results are consistent with data from transcriptomic analyses, the number of changed genes was equally higher for SK-N-MC cells incubated with BB than with RV, however, not mediating so efficacious protection (DSB Lab

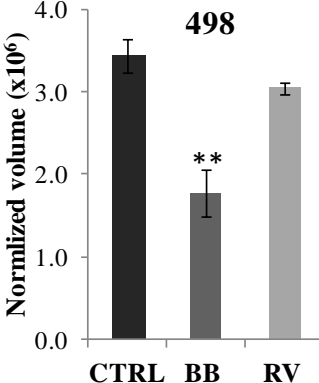
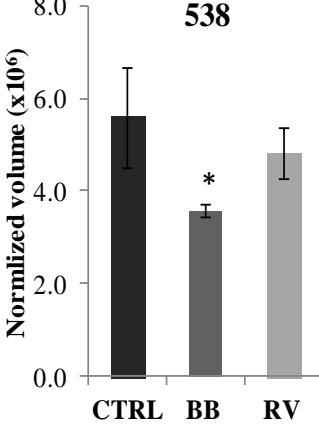
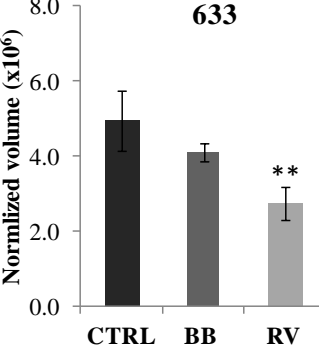
unpublished work and [23]). From proteomic analysis we may register that RV promotes protein changes to a lesser extent than BB.

The normalized volume for each protein spot differentially expressed from control and some of the characteristics of proteins such as pI and MW are described in Table 4.3, also their identification by MS (Table 4.3).

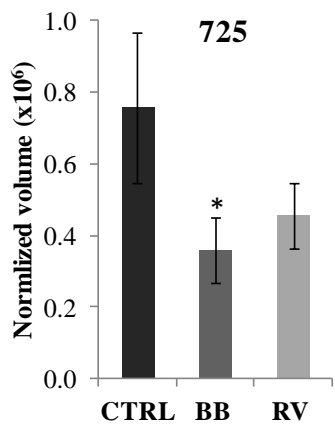
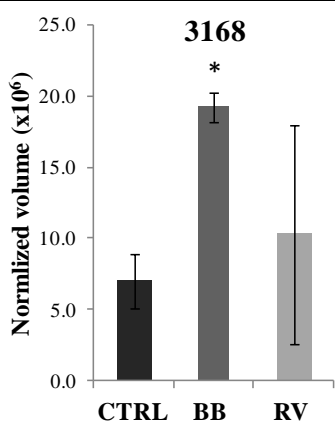
**Table 4.3** - Normalized volumes for protein spots in SK-N-MC cells treated with commercial blackberry (BB) and *R. vagabundus* (RV) differentially expressed from control (CTRL) and their characteristics (pI and MW (kDa)). Differences between treatments in relation to control are denoted as \* $p < 0.05$  \*\* $p < 0.01$  \*\*\* $p < 0.001$ .

Spots nr and normalized volumes	<i>m/z</i>	MS/MS sequence	Protein ID (accession number) <sup>i</sup>	MW (kDa) <sup>ii</sup>	pI <sup>iii</sup>
 <p>225</p>	-	-	-	74.8	9.4
 <p>272</p>	1933	DNHLLGTFDLTGIPPAPR	78 kDa glucose-regulated protein, <i>Homo sapiens</i> (P11021)	73.6 (70.0)	5.2 (4.8)
	1512	AKFEELNMDLFR			
	2164	IEIESFYEGEDFSETLTR			
	1887	VTHAVVTVPAYFNDAQR			

Spots nr and normalized volumes	<i>m/z</i>	MS/MS sequence	Protein ID (accession number) <sup>i</sup>	MW (kDa) <sup>ii</sup>	pI <sup>iii</sup>
 <p><b>247</b></p> <p>Normalized volume (x10<sup>6</sup>)</p> <p>CTRL BB RV</p>	-	-	-	71.6	9.2
 <p><b>3060</b></p> <p>Normalized volume (x10<sup>6</sup>)</p> <p>CTRL BB RV</p>	-	-	-	8.6	71.6
 <p><b>404</b></p> <p>Normalized volume (x10<sup>6</sup>)</p> <p>CTRL BB RV</p>	-	-	-	64.0	9.0

Spots nr and normalized volumes	<i>m/z</i>	MS/MS sequence	Protein ID (accession number) <sup>i</sup>	MW (kDa) <sup>ii</sup>	pI <sup>iii</sup>
 <p><b>498</b></p> <p>Normalized volume (x10<sup>6</sup>)</p> <p>CTRL BB RV</p>	-	-	-	60.5	7.0
 <p><b>538</b></p> <p>Normalized volume (x10<sup>6</sup>)</p> <p>CTRL BB RV</p>	1659	ALTVPELTQQVFDAK	Tubulin beta chain, <i>Homo sapiens</i> (P07437)	58.8 (52.0)	4.8 (4.8)
	2086	GHYTEGAELVDSVLDVVRK			
	2377	IREEYPDRIMNTFSVVPSPK			
	1229	ISEQFTAMFR			
	1572	LHFFMPGFAPLTSR			
	1039	YLTVAAVFR			
	1143	LAVNMVPFPR			
 <p><b>633</b></p> <p>Normalized volume (x10<sup>6</sup>)</p> <p>CTRL BB RV</p>	-	-	-	52.6	6.4



Spots nr and normalized volumes	<i>m/z</i>	MS/MS sequence	Protein ID (accession number) <sup>i</sup>	MW (kDa) <sup>ii</sup>	pI <sup>iii</sup>
 <p><b>725</b></p> <p>Normalized volume (x10<sup>6</sup>)</p> <p>CTRL BB RV</p>	-	-	-	46.0	7.2
 <p><b>3168</b></p> <p>Normalized volume (x10<sup>6</sup>)</p> <p>CTRL BB RV</p>	-	-	-	19.0	8.0


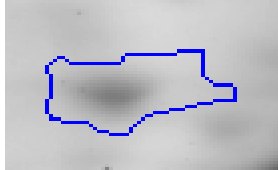
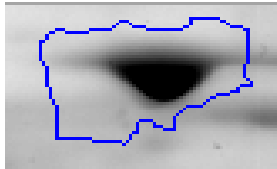
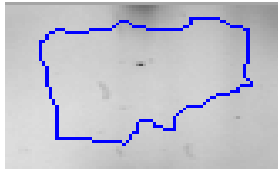
i) Protein identification according to the UniProt database (<http://www.uniprot.org>).

ii) Predicted MW (kDa) was obtained by using an ExPASy tool (<http://expasy.org>).

iii) Predicted pI and was obtained by using an ExPASy tool (<http://expasy.org>).

The 10 protein spots differentially expressed from control relatively to SK-N-MC cells incubated with BB and RV were analyzed by MS technique, and so far, 2 proteins were identified:  $\beta$ -tubulin (spot nr. 538) and GRP 78 (spot number 272) (Table 4.4).

**Table 4.4** - Protein identification by MS/MS and respectively gel images for control (CTRL) and commercial blackberry (BB).

Protein ID		
<b><math>\beta</math>-tubulin (538)</b>	<b>CTRL</b>	<b>BB</b>
		
<b>GRP 78 (272)</b>	<b>CTRL</b>	<b>BB</b>
		

The results showed that  $\beta$ -tubulin was statistically different from control and slightly downregulated (Fold change of 1.5) for cells incubated with BB.

$\beta$  and  $\alpha$ -tubulin are dynamic assembled polymers that compose microtubules (MTs), one of the components of the cytoskeleton that are present in all eukaryotic cells [80-82]. In neurons, MTs actively participate in the initial steps of neural polymerization, the organization of intracellular compartments and the remodeling of dendritic spines [82].

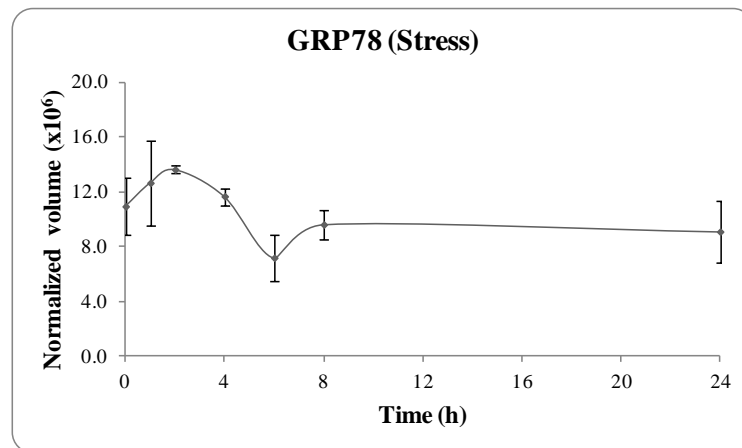
Tubulin receives diverse PTMs such as acetylation, tyrosination and phosphorylation that are implicated on the regulation of the neuronal MTs cytoskeleton. Processes like MTs dynamics, motor traffic and interaction between MTs and MTs associated proteins are regulated by tubulin PTMs, a contribution of these modifications to neurodegenerative disorders becomes a possibility that should be considered [80, 82].

Several studies have investigated the role of tubulin acetylation in AD, and suggested that changes in the levels of this PTM are involved in the pathogenesis of this disease [83].

Glucose regulated protein 78 (GRP 78) also referred as BiP or heat shock protein A5 is an important chaperone protein that is predominantly expressed in the endoplasmic reticulum (ER). This protein is described to be involved in various functions such as protein folding, endoplasmic reticulum calcium binding, cytoprotection, anti-apoptosis and autophagy inducer. This protein contains an ER stress elements in its promoters and are upregulated during ER stress [84, 85].

The results showed that GRP 78 (protein spot nr. 272) was statistically different from control (CTRL) being strongly downregulated (Fold change of 5) for cells incubated BB. Thus, we decided to observe the time course profile of this protein when cells were subjected to oxidative injury. The results obtained showed that over 6 h of stress the expression levels of this protein also decreased despite not statistically different (Fig. 4.5).

Then, the fact that GRP 78 was downregulated for cells when incubated with BB and also downregulated for 6 h, 8 h and 24 h of stress injury could mean that exposure of cells to components in the BB could be an initiating event that leads to protection against subsequent, potential lethal stimuli, known as preconditioning. This mechanism is clearly described for other heat shock proteins (HSP) [86, 87]. Also it is consistent with previous data that suggest preconditioning by digested berries metabolites [23].



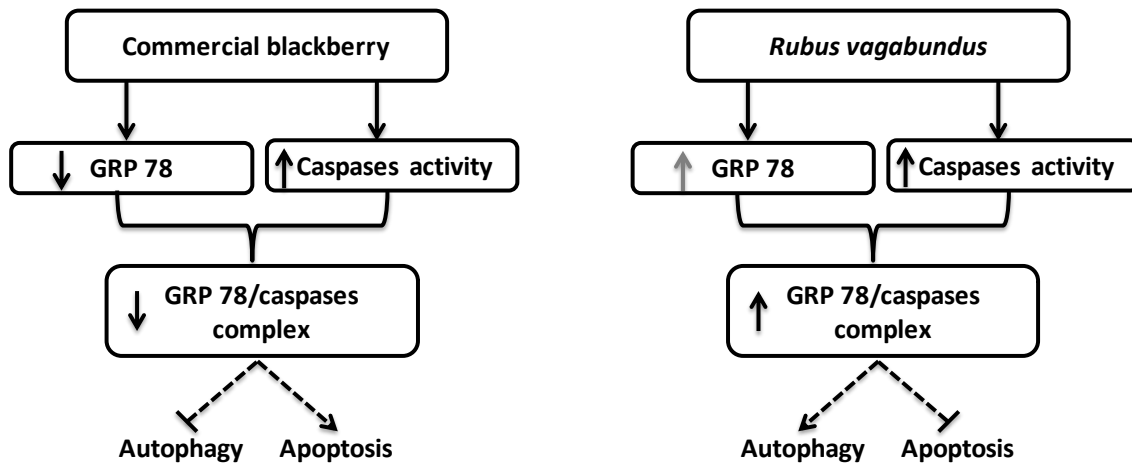
**Fig. 4.5** - Time course profile for the expression of GRP 78 in SK-N-MC cells when incubated for different periods of time with 300  $\mu$ M H<sub>2</sub>O<sub>2</sub> (0-24 h).

Some studies have demonstrated that GRP 78 forms a complex with caspase-7 and caspase-12 on the cytosolic side of the ER membrane, thereby blocking the main apoptosis-related machinery [84]. In previous works it was verified that BB and RV lead to caspases-3 and -7 activation (see annexes Fig. S2) [23].

The decrease in the expression of GRP 78 in cells incubated with BB could lead to apoptosis, since the complex GRP 78 with caspase-7 and -12 cannot be formed and the machinery of apoptosis will not be blocked. As so it is expected that cells incubated with BB will be protected from lethal injuries by controlled cell death mechanisms like apoptosis (Fig. 4.6 (A)).

In the case of cells incubated with RV there are no statistically differences from control, which suggest that GRP 78 could form a complex with caspases and beside caspases activation, the apoptosis was blocked (Fig. 4.6 (A)). The cross-talk between apoptosis and autophagy suggests

that RV could use autophagy as an alternative protective mechanism against possible lethal injuries (Fig. 4.6 (B)). Recently, it has been shown that ER stress could induce autophagy for cell survival in a neuroblastoma cell line [85].



**Fig. 4.6** - Scheme of the hypothetical effect of commercial blackberry (A) and *R.vagabundus* digested extracts (B) in caspases and GRP 78 expression in SK-N-MC cells.

Moreover, the importance of this protein in the physiological systems is reiterated by their participation on canonical pathways, such as Ubiquitin-Proteasomal pathway, because this pathway is central to the maintenance of homeostasis during stress by signaling damage or misfolded proteins for degradation and GRP 78 is an important chaperone that assist and regulate the correct folding of proteins [84, 88].

## 5. Final considerations and future perspectives

Neurodegenerative diseases are among the most complex human disorders. These devastating illnesses currently do not have any effective therapies or treatments, and are thus a social and economic encumber for modern society. Epidemiological studies showed a consistent relationship between the consumption of fruits and vegetables and a reduced risk of neurodegenerative diseases. Recently, berries upsurge as potential functional foods in the prevention of these diseases. One factor common to these diseases is oxidative stress, which is highly related with proteins, lipids, carbohydrates and nucleic acids damage, leading to cellular dysfunction and ultimately cell death [10, 16-19].

Evaluation of oxidative stress in our model of neurodegeneration by the described methods is a very helpful way to increase the knowledge about the pathways that can be compromised due to oxidative injury. The use of cellular models are a very helpful way to try to reproduce and manipulate molecular mechanisms that can be true for whole-organism systems, offering a faster approach to get trustable results and providing valuable biochemical information.

Deregulation of mechanisms underlying neurodegenerative disorders can be a hallmark in preventing disease progression and important to understand novel ways to fight extreme oxidative stress environments.

The analysis of the total proteome by 2DE revealed that oxidative stress in SK-N-MC cells resulted in altered expression of 12 protein spots from a total of 318. Since oxidative reactions are the main features during neurodegeneration we focused in some redox alterations, particularly proteins carbonylation and glutathionylation.

Responses at the protein carbonyl levels to stress over time suggest that cells produce early and late responses to oxidative injury. On the other hand, the pattern of glutathionylated proteins obtained for SK-N-MC cells treated with H<sub>2</sub>O<sub>2</sub> showed that only the positive control presents a glutathionylated protein, for the remaining incubation times with H<sub>2</sub>O<sub>2</sub> no polypeptide appears glutathionylated. However, the avidity for glutathionylation increases after 4 h of stress. Previous results from DSB Lab showed that free GSH levels start to decrease after 4 h of H<sub>2</sub>O<sub>2</sub> incubation, this decrease is consistent with the glutathionylation avidity increases detected. Further studies should be done to identify this polypeptide.

The ability to visualize proteins on high resolution 2DE immunoblots offers significant advantages over 1DE molecular weight separation, so in future work we will try to implement 2DE immunoblots for both redox proteomic targets. Moreover, it becomes clear that could be interesting to fractionate our sample; this allows to reduce the complexity of protein/peptide mixtures and to separate various groups of proteins for subsequent analysis [57, 75, 77]

Endemic blackberry species revealed to be a promising source of metabolites with neuroprotection capabilities. Although the number of altered protein spots was higher for cells incubated with BB than for RV, the former not mediate so efficacious protection [23].

From 9 statistically different protein spots detected in cells incubated with BB, only  $\beta$ -tubulin and GRP78 were until now identified by mass spectrometry.

Tubulin can receive diverse PTMs such as acetylation, tyrosination and phosphorylation that are implicated on the regulation of the neuronal MTs cytoskeleton. Processes like MTs dynamics, motor traffic and interaction between MTs and MTs associated proteins are regulated by tubulin PTMs, a contribution of these modifications to neurodegenerative disorders becomes a possibility that should be considered [80, 82].

GRP 78 is described to be involved in various functions such as protein folding, endoplasmic reticulum calcium binding, cytoprotection, anti-apoptosis and autophagy inducer. The decrease in the expression of GRP 78 in cells incubated with BB could lead to apoptosis, since the complex GRP 78 with caspase-7 and -12 cannot be formed and the machinery of apoptosis will not be blocked. As so, it is expected that cells incubated with BB probably will be protected from lethal injuries by controlled cell death mechanisms like apoptosis.

In the case of cells incubated with RV there are no statistically differences from control, which suggest that GRP 78 could form a complex with caspases and beside caspases activation, the apoptosis was blocked. The cross-talk between apoptosis and autophagy suggests that RV could use autophagy as an alternative protective mechanism against possible lethal injuries.

However, further studies should be performed, to understand the role of these two proteins in neuroprotection and validate the mechanisms proposed.

Further studies involving the selection of sub proteomes will be necessary to have a better understanding of the mechanisms underlying the neuroprotective effects of berries.

## 6. Bibliography

1. Barnham, K.J., Masters, C.L., and Bush, A.I., *Neurodegenerative diseases and oxidative stress*. Nat Rev Drug Discov, **2004**. 3(3): p. 205-214.
2. Bains, J.S., and Shaw, C.A., *Neurodegenerative disorders in humans: the role of glutathione in oxidative stress-mediated neuronal death*. Brain Res Brain Res Rev, **1997**. 25(3): p. 335-358.
3. Shulka, V., Mishra S.K., and Pant, H.C., *Oxidative stress in neurodegeneration*. Adv Pharmacol Sci, **2011**. doi:10.1155/2011/572634.
4. Butterfield, D.A., *Proteomics: a new approach to investigate oxidative stress in Alzheimer's disease brain*. Brain Res, **2004**. 12: p. 1-2.
5. Sultana, R., and Butterfield, D.A., *Role of oxidative stress in the progression of Alzheimer's disease*. J Alzheimers Dis, **2010**. 19(1): p. 341-353.
6. Katzman, R., and Saitoh, T., *Advances in Alzheimer's disease*. The FASEB Journal, **1991**. 5(3): p. 278-286.
7. Butterfield, D.A., Perluigi, M., and Sultana, R., *Oxidative stress in Alzheimer's disease brain: new insights from redox proteomics*. Eur J Pharmacol, **2006**. 545(1): p. 39-50.
8. Muller, T., Tribl, F., Hamacher, M., Hall, A., Meyer, H., and Marcus, K., *Proteomics of the nervous system*, in Wiley-Blackwell. **2008**. p. 209-210.
9. Gandhi, S., and Abramov, A. Y., *Mechanism of oxidative stress in neurodegeneration*. Oxi Med Cell Long, **2012**. doi:10.1155/2012/428010.
10. Sultana, R., Newman, S.F., Butterfield, D.A., *Redox Proteomics: Application to Age-Related Neurodegenerative Disorders*, Wiley-Blackwell, 2008. p. 255-257
11. Du, J. and Gebicki, J.M., *Proteins are major initial cell targets of hydroxyl free radicals*. Int J Biochem Cell Biol, **2004**. 36(11): p. 2334-2343.
12. Nunomura, A., Honda, K., Takeda, A., Hirai, K., Zhu, X., Smith, M., A., and Perry, G., *Oxidative damage to RNA in neurodegenerative diseases*. J Biomed Biotechnol, **2006**. doi 10.1155/JBB/2006/82323.
13. Halliwell, B., *Oxidative stress and neurodegeneration: where are we now?* J Neurochem, **2006**. 97(6): p. 1634-1658.
14. Biedler, J. L., Lawrence, H., and Spengler, B. A., *Morphology and growth, tumorigenicity, and cytogenetics of human neuroblastoma cells in continuous culture*. Cancer Res, **1973**. 33: p. 2643-2652.
15. Tavares, L., Figueira, I., Macedo, D., McDougall, G. J., Leitão, M. C., Vieira, H. L. A., Stewart, D., Alves, P. M., Ferreira, R. B., and Santos, C. N., *Neuroprotective effect of blackberry (Rubus sp.) polyphenols is potentiated after simulated gastrointestinal digestion*. Food Chem, 2011. 131(4): p. 1443-1452
16. Paredes-López, O., Cervantes-Ceja, M. L., Vigna-Pérez, M., and Hernández-Pérez, T., *Berries: improving human health and healthy aging, and promoting quality life - a review*. Plant Foods Hum Nutr, **2010**. 65(3): p. 299-308.
17. de Rijk, M. C., Breteler, M. M., den Breeijen, J. H., Launer, L. J., Grobbee, D. E., van der Meché, F. G., and Hofman, A., *Dietary antioxidants and Parkinson disease. The Rotterdam study*. Arch Neurol, **1997**. 54(6): p. 762-765.
18. Dai, Q., Borenstein, A. R., Wu, Y., Jackson, J. C., and Larson, E. B., *Fruit and vegetable juices and Alzheimer's disease: the Kame project*. Am J Med, **2006**. 119(9): p. 751-759.

19. Di Matteo, V. and Esposito, E., *Biochemical and therapeutic effects of antioxidants in the treatment of Alzheimer's disease, Parkinson's disease, and amyotrophic lateral sclerosis*. Curr Drug Targets CNS Neurol Disord, **2003**. 2(2): p. 95-107.
20. Dai, J., Patel, J. D., and Mumper, R. J., *Characterization of blackberry extract and its antiproliferative and anti-inflammatory properties*. J Med Food, **2007**. 10(2): p. 258-265.
21. Wang, S. Y. and Jiao, H., *Scavenging capacity of berry crops on superoxide radicals, hydrogen peroxide, hydroxyl radicals, and singlet oxygen*. J Agric Food Chem, **2000**. 48(11): p. 5677-5684.
22. Shukitt-Hale, B., Cheng, V., and Joseph, J., *Effects of blackberries on motor and cognitive function in aged rats*. Nutr Neurosci, **2009**. 12(3): p. 135-140.
23. Tavares, L., McDougall, G. J., Fortalezas, S., Stewart, D., Ferreira, R. B., and Santos, C. N., *Neuroprotective effects of digested polyphenols from wild blackberry species*. Eur J Nutr, **2012**. (DOI) 10.1007/s00394-012-0307-7.
24. Koli, R., Erlund, I., Julia, A., Marniemi, J., Mattila, P., and Alfthan, G., *Bioavailability of various polyphenols from a diet containing moderate amounts of berries*. J Agric Food Chem, **2010**. 58(7): p. 3927-3932.
25. Zhao, Z. and Moghadasian, M.H., *Chemistry, natural sources, dietary intake and pharmacokinetic properties of ferulic acid: A review*. Food Chem, **2008**. 109(4): p. 691-702.
26. Lafay, S. and Gil-Izquierdo, A., *Bioavailability of phenolic acids*. Phytochem Rev, **2008**. 7(2): p. 301-311.
27. McGhie, T. K., and Walton, M. C., *The bioavailability and absorption of anthocyanins: Towards a better understanding*. Mol Nutr Food Res, **2007**. 51(6): p. 702-713.
28. McDougall, G.J., Dobson, P., Smith, P., Blake, A., and Stewart, D., *Assessing potential bioavailability of raspberry anthocyanins using an in vitro digestion system*. J Agric Food Chem, **2005**. 53(15): p. 5896-5904.
29. Aura, A. M., *In vitro digestion models for dietary phenolic compounds*, PhD Thesis, **2005**. Helsinki University, Finland.
30. Gauci, V., Wright, E., and Coorssen, J., *Quantitative proteomics: assessing the spectrum of in-gel protein detection methods*. J Chem Biol, **2011**. 4(1): p. 3-29.
31. Rotilio, D., Della Corte, A., D'Imperio, M., Coletta, W., Marcone, S., Silvestri, C., Giordano, L., Di Michele, M., Donati, M. B., *Proteomics: bases for protein complexity understanding*. Thromb Res, **2012**. 129(3): p. 257-262.
32. O'Farrell, P. H., *High resolution two-dimensional electrophoresis of proteins*. J Biol Chem, **1975**. 250(10): p. 4007-4021.
33. Fenn, J. B., Mann, M., Meng, C. K., Wong, S. F., Whitehouse, C. M., *Electrospray ionization for mass spectrometry of large biomolecules*. Science, **1989**. 246(4926): p. 64-71.
34. Gygi, S. P., Rist, B., Gerber, S. A., Turecek, F., Gelb, M. H., Aebersold, R., *Quantitative analysis of complex protein mixtures using isotope-coded affinity tags*. Nat Biotech, **1999**. 17(10): p. 994-999.
35. D'Imperio, M., Della Corte, A., Facchiano, A., Di Michele, M., Ferrandina, G., Donati, M. B., Rotilio, D. *Standardized sample preparation phases for a quantitative measurement of plasma peptidome profiling by MALDI-TOF*, **2010**. J Proteomics. 73(7): p. 1355-1367.
36. Vercauteren, F. G., Arckens, L., and Quirion, R., *Applications and current challenges of proteomic approaches, focusing on two-dimensional electrophoresis*. Amino Acids, **2007**. 33(3): p. 405-414.



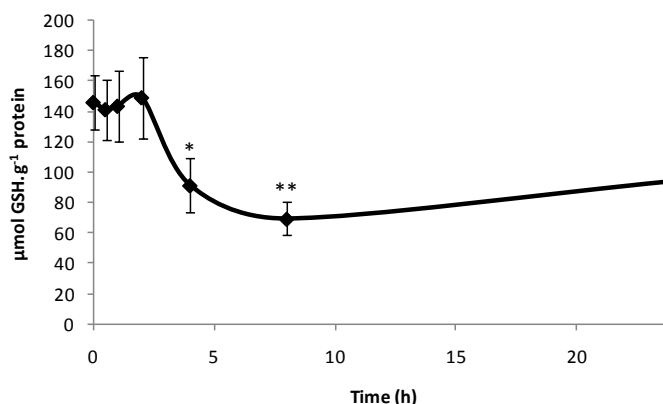
37. Gromov, P., I. Gromova, and J.E. Celis, *Proteomic Analysis by Two-Dimensional Polyacrylamide Gel Electrophoresis*, in *Proteomics for Biological Discovery*. **2006**, John Wiley & Sons, Inc. p. 19-46.
38. Rabilloud, T., *Two-dimensional gel electrophoresis in proteomics: old, old fashioned, but it still climbs up the mountains*. *Proteomics*, **2002**. 2(1): p. 3-10.
39. O'Farrell, P.Z., Goodman, H. M., and O'Farrell, P. H., *High resolution two-dimensional electrophoresis of basic as well as acidic proteins*. *Cell*, **1977**. 12(4): p. 1133-1141.
40. Butterfield, D. A., and Sultana, R., *Redox proteomics: understanding oxidative stress in the progression of age-related neurodegenerative disorders*. *Expert Rev Proteomics*, **2008**. 5(2): p. 157-160.
41. Tetik, S., Kaya, K., Demir, M., Eksioglu-Demiralp, E., and Yardimci, T., *Proteins as sensitive biomarkers of human conditions associated with oxidative stress*, in *Redox Proteomics*. **2006**, John Wiley & Sons, Inc. p. 485-525.
42. Butterfield, D. A., Perluigi, M., Reed, T., Muharib, T., Hughes, C. P., Robinson, R. A., and Sultana, R., *Redox proteomics in selected neurodegenerative disorders: from its infancy to future applications*. *Antioxid Redox Signal*, **2012**. doi/abs/10.1089/ars.2011.4109.
43. Sheehan, D., McDonagh, B., and Barcena, J. A., *Redox proteomics*. *Expert Rev Proteomics*, **2010**. 7(1): p. 1-4.
44. Davies, M.J., *The oxidative environment and protein damage*. *Biochim Biophys Acta*, **2005**. 17(2): p. 93-109.
45. D'Alessandro, A., Rinalducci, S., and Zolla, L., *Redox proteomics and drug development*. *J Proteomics*, **2011**. 74(12): p. 2575-2595.
46. David, S., *Detection of redox-based modification in two-dimensional electrophoresis proteomic separations*. *Biochem Biophys Res Commun*, **2006**. 349(2): p. 455-462.
47. Biswas, S., Chida, A. S., and Rahman, I., *Redox modifications of protein-thiols: emerging roles in cell signaling*. *Biochem Pharmacol*, **2006**. 71(5): p. 551-564.
48. Radak, Z., Zhao, Z., Goto, S., and Koltai, E., *Age-associated neurodegeneration and oxidative damage to lipids, proteins and DNA*. *Mol Aspects Med*, **2011**. 32(4-6): p. 305-315.
49. Ghezzi, P. and Bonetto, V., *Redox proteomics: identification of oxidatively modified proteins*. *Proteomics*, **2003**. 3(7): p. 1145-1153.
50. Dalle-Donne, I., Rossi, R., Giustarini, D., Milzani, A., and Colombo, R., *Protein carbonyl groups as biomarkers of oxidative stress*. *Clin Chim Acta*, **2003**. 329(1-2): p. 23-38.
51. Levine, R. L., Williams, J. A., Stadtman, E. R., and Shacter, E., *Carbonyl assays for determination of oxidatively modified proteins*. *Methods Enzymol*, **1994**. 233: p. 346-357.
52. Dalle-Donne, I., Rossi, R., Colombo, G., Giustarini, D., and Milzani, A., *Protein S-glutathionylation: a regulatory device from bacteria to humans*. *Trends Biochem Sci*, **2009**. 34(2): p. 85-96.
53. Dalle-Donne, I., Colombo, G., Gagliano, N., Colombo, R., Giustarini, D., Rossi, R., and Milzani, A., *S-Glutathiolation in life and death decisions of the cell*. *Free Radic Res*, **2011**. 45(1): p. 3-15.
54. Newman, S. F., Sultana, R., Perluigi, M., Coccia, R., Cai, J., Pierce, W. M., Klein, J. B., Turner, D. M., and Butterfield, D. A., *An increase in S-glutathionylated proteins in the Alzheimer's disease inferior parietal lobule, a proteomics approach*. *J Neurosci Res*, **2007**. 85(7): p. 1506-1514.
55. Dalle-Donne, I., Rossi, R., Giustarini, D., Colombo, R., and Milzani, A., *S-glutathionylation in protein redox regulation*. *Free Radic Biol Med*, **2007**. 43(6): p. 883-898.

56. Pastore, A., and Piemonte, F., *S -Glutathionylation signaling in cell biology: progress and prospects*. Eur J Pharm Sci, **2012**. 46(5): p. 279-292.
57. Hill, B. G., Ramana, K. V., Cai, J., Bhatnagar, A., and Srivastava, S. K., *Measurement and identification of S-glutathiolated proteins*. Methods Enzymol, **2010**. 473: p. 179-197.
58. Cohn, V.H., and Lyle, J., *A fluorometric assay for glutathione*. Anal Biochem, **1966**. 14(3): p. 434-440.
59. Tavares, L., Fortalezas, S., Carrilho, C., McDougall, G. J., Stewart, D., Ferreira, R. B., and Santos, C., *Antioxidant and antiproliferative properties of strawberry tree tissues*. J Berry Res, **2010**. 1: p. 3-12.
60. McDougall, G. J., Fyffe, S., Dobson, P., Stewart, D., *Anthocyanins from red wine - Their stability under simulated gastrointestinal digestion*. Phytochem, **2005**. 66(21): p. 2540-2548.
61. Bensadoun, A., and Weinstein, D., *Assay of proteins in the presence of interfering materials*. Anal Biochem, **1976**. 70(1): p. 241-250.
62. Markwell, M. A., Haas, S. M., Bieber, L. L., and Tolbert, N. E., *A modification of the Lowry procedure to simplify protein determination in membrane and lipoprotein samples*. Anal Biochem, **1978**. 87(1): p. 206-210.
63. Barata, D.B., "Polifenóis com importância em Neurodegeneração: a via da ubiquitina/proteassoma" in ITQB. **2007**, MsC Thesis, FCT-UNL, Lisbon.
64. Laemmli, U. K., *Cleavage of structural proteins during the assembly of the head of bacteriophage T4*. Nature, **1970**. 227(5259): p. 680-685.
65. Esteves, S. T. L., *Análise Proteómica das fracções subcelulares de uma linha de neuroblastomas humanos*, 2009. MsC Thesis, ISA, UTL, Lisbon.
66. Neuheff, V., Arold, N., Taube, D., and Ehrhardt, W., *Improved staining of proteins in polyacrylamide gels including isoelectric focusing gels with clear background at nanogram sensitivity using Coomassie Brilliant Blue G-250 and R-250*. Electrophoresis, **1988**. 9(6): p. 255-262.
67. Gorg, A., Weiss, W., and Dunn, M. J., *Current two-dimensional electrophoresis technology for proteomics*. Proteomics, **2004**. 4(12): p. 3665-3685.
68. Progenesis SameSpots Tutorial. 2012 18.04.2012]; Available from: <http://www.nonlinear.com/products/progenesis/samespots/analysis-workflow/>.
69. Shevchenko, A., Tomas, H., Havlis, J., Olsen, J. V., and Mann, M., *In-gel digestion for mass spectrometric characterization of proteins and proteomes*. Nat Protoc, **2006**. 1(6): p. 2856-2860.
70. Swerdlow, P. S., Finley, D. , and Varshavsky, A., *Enhancement of immunoblot sensitivity by heating of hydrated filters*. Anal Biochem, **1986**. 156(1): p. 147-153.
71. Kand'ár, R., Záková, P., Lotková, H., Kucera, O., and Cervinková, Z., *Determination of reduced and oxidized glutathione in biological samples using liquid chromatography with fluorimetric detection*. J Pharm Biomed Anal, **2007**. 43(4): p. 1382-1387.
72. Hissin, P. J., and Hilf, R., *A fluorometric method for determination of oxidized and reduced glutathione in tissues*. Anal Biochem, **1976**. 74(1): p. 214-226.
73. Quackenbush, J., *Microarray data normalization and transformation*. Nat Genet, **2002**. 32: p. 496-501.
74. Whittemore, E. R., Loo, D. T., Watt, J. A., and Cotman, C. W., *A detailed analysis of hydrogen peroxide-induced cell death in primary neuronal culture*. Neurosci, **1995**. 67(4): p. 921-932.

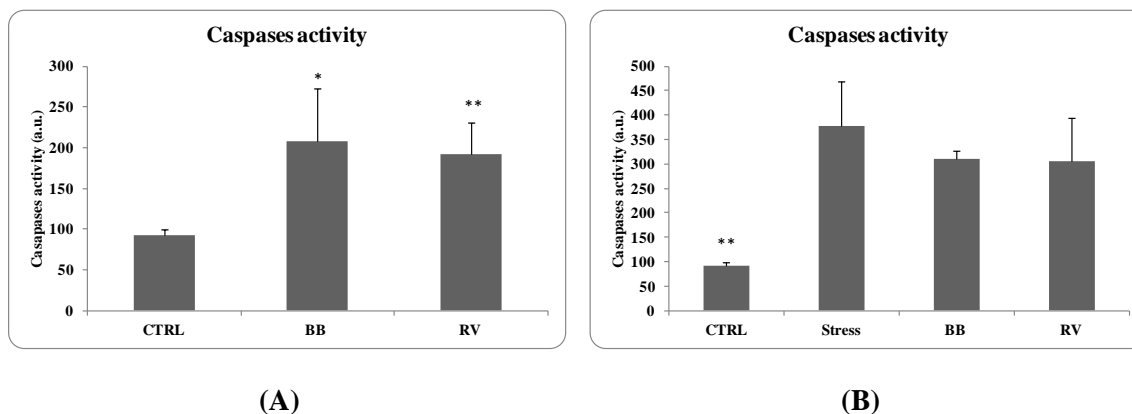
75. Medvedev, A., Kopylov, A., Buneeva, O., Zgoda, V., Archakov, A., *Affinity-based proteomic profiling: problems and achievements*. Proteomics, **2012**. 12(4-5): p. 621-637.
76. Sultana, R., Perluigi, M., and Butterfield, D. A., *Protein oxidation and lipid peroxidation in brain of subjects with Alzheimer's disease: insights into mechanism of neurodegeneration from redox proteomics*. Antioxid Redox Signal, **2006**. 8(11-12): p. 2021-2037.
77. Conrad, C. C., Choi, J., Malakowsky, C. A., Talent, J. M., Dai, R., Marshall, P., and Gracy, R. W., *Identification of protein carbonyls after two-dimensional electrophoresis*. Proteomics, **2001**. 1(7): p. 829-834.
78. Harding, J. J., *Free and protein-bound glutathione in normal and cataractous human lenses*. Biochem J, **1970**. 117(5): p. 957-960.
79. Hill, B. G., and Bhatnagar, A., *Protein S-glutathiolation: Redox-sensitive regulation of protein function*. J Mol Cell Cardiol, **2012**. 52(3): p. 559-567.
80. Fukushima, N., Furuta, D., Hidaka, Y., Moriyama, R., and Tsujiuchi, T., *Post-translational modifications of tubulin in the nervous system*. J Neurochem, **2009**. 109(3): p. 683-693.
81. Hammond, J. W., Cai, D., and Verhey, K. J., *Tubulin modifications and their cellular functions*. Curr Opin Cell Biol, **2008**. 20(1): p. 71-76.
82. Janke, C., and Kneussel, M., *Tubulin post-translational modifications: encoding functions on the neuronal microtubule cytoskeleton*. Trends Neurosci, **2010**. 33(8): p. 362-372.
83. Perez, M., Santa-Maria, I., Gomez de Barreda, E., Zhu, X., Cuadros, R., Cabrero, J. R., Sanchez-Madrid, F., Dawson, H. N., Vitek, M. P., Perry, G., Smith, M. A., and Avila, J., *Tau – an inhibitor of deacetylase HDAC6 function*. J Neurochem, **2009**. 109(6): p. 1756-1766.
84. Weng, W. C., Lee, W. T., Hsu, W. M., Chang, B. E., and Lee, H., *Role of glucose-regulated protein 78 in embryonic development and neurological disorders*. J Formos Med Assoc, **2011**. 110(7): p. 428-437.
85. Ogata, M., Hino, S., Saito, A., Morikawa, K., Kondo, S., Kanemoto, S., Murakami, T., Taniguchi, M., Tanii, I., Yoshinaga, K., Shiosaka, S., Hammarback, J. A., Urano, F., and Imaizumi, K., *Autophagy is activated for cell survival after endoplasmic reticulum stress*. Mol Cell Biol, **2006**. 26(24): p. 9220-9231.
86. Garnier, P., Ying, W., and Swanson, R. A., *Ischemic preconditioning by caspase cleavage of poly(ADP-ribose) polymerase-1*. J Neurosci, **2003**. 23(22): p. 7967-7973.
87. McLaughlin, B., Hartnett, K. A., Erhardt, J. A., Legos, J. J., White, R. F., Barone, F. C., Aizenman, E., *Caspase 3 activation is essential for neuroprotection in preconditioning*. Proc Natl Acad Sci U S A, **2003**. 100(2): p. 715-720.
88. Mathew, A., S.K. Mathur, and R.I. Morimoto, *Heat Shock Response and Protein Degradation: Regulation of HSF2 by the Ubiquitin-Proteasome Pathway*. Mol Cell Biol, **1998**. 18(9): p. 5091-5098.



## 7. Annexes



**Fig. S1** - Thiols time course profile of stressed SK-N-MC cells: GSH. SK-N-MC cells were submitted to an oxidative stress (300μM H<sub>2</sub>O<sub>2</sub>) for different incubation periods (0-24 h) and protein cellular extracts were derivatized and quantified by HPLC with fluorescence detector. Glutathione-OPA adduct was monitored at excitation and emission wavelengths of 350 and 420 nm, respectively. Quantifications of GSH were normalized for total protein content. Represented values are the averages ± S.D. of at least three independent determinations. Differences between treatments in relation to control are denoted as \**p*<0.05 \*\**p*<0.01. Data provided by a colleague from DSB Lab.



**Fig. S2** - (A) Caspase-3 and -7 activity from SK-N-MC cells when incubated with 0.5 μg GAE mL<sup>-1</sup> of commercial blackberry (BB) or *R.vagabundus* (RV); Differences between treatments in relation to control (CTRL) are denoted as \**p*<0.05 \*\**p*<0.01 (B) Caspase-3 and -7 activity from SK-N-MC cells when pre-incubated with 0.5 μg GAE mL<sup>-1</sup> of commercial blackberry (BB) or *R.vagabundus* (RV) and then submitted to oxidative stress (300 μM H<sub>2</sub>O<sub>2</sub>); Differences between treatments in relation to oxidative stress (Stress) are denoted as \*\**p*<0.01. Data provided by a DSB Lab colleague.